8

Rolling contact of elastic bodies

8.1 Micro-slip and creep

In Chapter 1 *rolling* was defined as a relative angular motion between two bodies in contact about an axis parallel to their common tangent plane (see Fig. 1.1). In a frame of reference which moves with the point of contact the surfaces 'flow' through the contact zone with tangential velocities $\mathbf{V}_1$ and $\mathbf{V}_2$. The bodies may also have angular velocities ω_{z1} and ω_{z2} about their common normal. If $\mathbf{V}_1$ and $\mathbf{V}_2$ are unequal the rolling motion is accompanied by *sliding* and if ω_{z1} and ω_{z2} are unequal it is accompanied by *spin.* When rolling occurs without sliding or spin the motion is often referred to as 'pure rolling'. This term is ambiguous, however, since absence of apparent sliding does not exclude the transmission of a tangential force Q, of magnitude less than limiting friction, as exemplified by the driving wheels of a vehicle. The terms *free rolling* and *tractive rolling* will be used therefore to describe motions in which the tangential force Q is zero and non-zero respectively.

We must now consider the influence of elastic deformation on rolling contact. First the normal load produces contact over a finite area determined by the Hertz theory. The specification of 'sliding' is now not so straightforward since some contacting points at the interface may 'slip' while others may 'stick'. From the discussion of incipient sliding in §7.2, we might expect this state of affairs to occur if the interface is called upon to transmit tangential tractions. A difference between the tangential strains in the two bodies in the 'stick' area then leads to a small apparent slip which is commonly called *creep.* The way in which creep arises may be appreciated by the example of a deformable wheel rolling on a relatively rigid plane surface. If, owing to elastic deformation under load, the tangential (i.e. circumferential) strain in the wheel is tensile, the surface of the wheel is stretched where it is in sticking contact with the plane. The wheel then behaves as though it had an enlarged circumference and, in one

revolution, moves forward a distance greater than its undeformed perimeter by a fraction known as the *creep ratio.* If the tangential strain in the wheel is compressive the effect is reversed.

The phenomenon of creep was described by Reynolds (1875) in a remarkably perceptive paper. He recognised that the contact region would be divided into stick and micro-slip zones in a manner determined by the interplay of friction forces and elastic deformation, and supported his arguments by creep measurements using a rubber cylinder rolling on a metal plane and vice versa.†

The boundary conditions which must be satisfied in the stick and micro-slip regions of rolling contact will now be developed. In our coordinate system we shall take rolling to be about the y-axis so that, in the absence of deformation and sliding, material particles of each surface flow through the contact region parallel to the x-axis with a common velocity V known as the rolling speed. In addition the bodies may have angular velocities ω_{z1} and ω_{z2} due to spin. The application of tangential tractions and the resulting deformation introduce creep velocities $\delta\mathbf{V}_1$ and $\delta\mathbf{V}_2$, each having components in both the x and y directions, which are small compared with the rolling speed V. This is the Eulerian view in which the material moves while the field of deformation remains fixed in space. The velocity of a material element is also influenced by the state of strain in the deformed region. If the components of tangential elastic displacement at a surface point (x, y) are $\bar{u}_x(x, y, t)$ and $\bar{u}_y(x, y, t)$ the 'undeformed' velocity is modified by the components

$$\frac{\mathrm{d}\bar{u}_x}{\mathrm{d}t} = V\frac{\partial\bar{u}_x}{\partial x} + \frac{\partial\bar{u}_x}{\partial t}$$

and

$$\frac{\mathrm{d}\bar{u}_y}{\mathrm{d}t} = V\frac{\partial\bar{u}_y}{\partial x} + \frac{\partial\bar{u}_y}{\partial t}$$

Hence the resultant particle velocities at a general surface point, taking into account creep, spin and deformation, are given by the expressions:

$$v_x(x, y) = V + \delta V_x - \omega_z y + V\frac{\partial\bar{u}_x}{\partial x} + \frac{\partial\bar{u}_x}{\partial t} \qquad (8.1a)$$

† Reynolds found that a rubber cylinder moved forward more than its undeformed circumference in one revolution and hence deduced that the circumferential strain was *tensile.* He explained this result by the influence of Poisson's ratio on the radial *compressive* strain produced by the normal load. However, it follows from the Hertz theory (1882*a*) that the tangential strain is, in general, *compressive* and for an incompressible material like rubber is zero. The explanation for the anomaly lies in Reynolds' use of a relatively thin rubber cover on a rigid hub for his deformable roller. In these circumstances the tangential strains in the cover are tensile and consistent with the experiments (see Bentall & Johnson, 1967).

and

$$v_y(x,y) = \delta V_y + \omega_z x + V\frac{\partial \bar{u}_y}{\partial x} + \frac{\partial \bar{u}_y}{\partial t} \tag{8.1b}$$

If the strain field does not change with time, which would be the case in *steady rolling* (i.e. uniform motion under constant forces), the final terms in these expressions vanish. The terms $(\partial \bar{u}_x/\partial x)$ and $(\partial \bar{u}_y/\partial x)$ arise from the state of strain in the surface, which can be found if the surface tractions are known. They are necessarily small compared with unity. The velocities of micro-slip between contacting points in steady rolling are then given by

$$\begin{aligned} \dot{s}_x(x,y) &\equiv v_{x1} - v_{x2} \\ &= (\delta V_{x1} - \delta V_{x2}) - (\omega_{z1} - \omega_{z2})y + V\left(\frac{\partial \bar{u}_{x1}}{\partial x} - \frac{\partial \bar{u}_{x2}}{\partial x}\right) \end{aligned} \tag{8.2a}$$

and

$$\begin{aligned} \dot{s}_y(x,y) &\equiv v_{y1} - v_{y2} \\ &= (\delta V_{y1} - \delta V_{y2}) + (\omega_{z1} - \omega_{z2})x + V\left(\frac{\partial \bar{u}_{y1}}{\partial x} - \frac{\partial \bar{u}_{y2}}{\partial x}\right) \end{aligned} \tag{8.2b}$$

For an elliptical contact area of semi-axes a and b, we rewrite (8.2) in non-dimensional form to give

$$\dot{s}_x/V = \xi_x - \psi y/c + \left(\frac{\partial \bar{u}_{x1}}{\partial x} - \frac{\partial \bar{u}_{x2}}{\partial x}\right) \tag{8.3a}$$

$$\dot{s}_y/V = \xi_y + \psi x/c + \left(\frac{\partial \bar{u}_{y1}}{\partial x} - \frac{\partial \bar{u}_{y2}}{\partial x}\right) \tag{8.3b}$$

where $\xi_x \equiv (\delta V_{x1} - \delta V_{x2})/V$ and $\xi_y \equiv (\delta V_{y1} - \delta V_{y2})/V$ are the *creep ratios* ψ is the non-dimensional *spin parameter* $(\omega_{z1} - \omega_{z2})c/V$ and $c = (ab)^{1/2}$.

In a stick region

$$\dot{s}_x = \dot{s}_y = 0 \tag{8.4}$$

In addition, the resultant tangential traction must not exceed its limiting value, viz.:

$$|q(x,y)| \leqslant \mu p(x,y) \tag{8.5}$$

where μ is the coefficient of limiting friction.

In a slip region, on the other hand,

$$|q(x,y)| = \mu p(x,y) \tag{8.6}$$

and the direction of q must oppose the slip velocity, viz.:

$$\frac{\mathbf{q}(x,y)}{|q(x,y)|} = -\frac{\dot{\mathbf{s}}(x,y)}{|\dot{s}(x,y)|} \tag{8.7}$$

https://doi.org/10.1017/CBO9781139171731.009 Published online by Cambridge University Press

Equations (8.4)–(8.7) specify the boundary conditions at the interface of two bodies in steady rolling contact; the first two apply in that part of the contact area where there is no slip and the second two apply in the zone of micro-slip. It will be appreciated from the examples which we shall discuss in the remainder of this chapter that one of the chief difficulties of such problems lies in finding the configurations of the stick and slip zones. In this respect the conditions at the boundaries of the contact area are significant. At the leading edge, where the material is flowing into the contact, the strain and hence the velocity must be continuous across the boundary. We saw in §2.5 that a discontinuity in tangential traction q at the boundary leads to a singularity in surface strain just outside the contact. It follows, therefore, that $q = 0$ at all points on the leading edge of the contact. The situation at the trailing edge is different. If we postulate a coefficient of friction sufficiently high to prevent any slip until the material emerges from the trailing edge, such that there is a discontinuity in traction, then the instantaneous change in strain and hence velocity at that point implies that, in reality, some of the stored elastic energy is irreversibly dissipated. For such a situation to arise in reverse at the leading edge would clearly contravene thermodynamic principles.

Creep of an elastic belt

The most elementary example of creep and micro-slip in rolling contact is provided by a flexible elastic belt which is transmitting a torque M between two equal pulleys (see Fig. 8.1). If $T_1 (= T_0 + t)$ and $T_2 (= T_0 - t)$ are the tensions on the tight side and slack side respectively,

$$T_1 - T_2 = 2t = M/R \tag{8.8}$$

The belt slips on each pulley over an arc $R\phi$ given by the capstan formula:

$$e^{\mu\phi} = \frac{T_1}{T_2} = \frac{1 + M/2RT_0}{1 - M/2RT_0} \tag{8.9}$$

where it is assumed that the torque M is sufficiently small for the arc of slip to be less than the arc of the belt (i.e. $\phi < \pi$). The question now arises: where is the slip arc located on each pulley? The tensile strain in an elastic belt of extensibility λ is given by

$$\epsilon = \lambda T$$

so that an element of belt of unstretched length $\mathrm{d}x$, when under tension, has length $\mathrm{d}l = (1 + \epsilon)\,\mathrm{d}x$. The velocity of the element is thus given by

$$v = \frac{\mathrm{d}l}{\mathrm{d}t} = (1 + \epsilon)\frac{\mathrm{d}x}{\mathrm{d}t} = (1 + \lambda T)V \tag{8.10}$$

where $V (= \mathrm{d}x/\mathrm{d}t)$ is the 'unstretched' velocity of the belt. This expression is

https://doi.org/10.1017/CBO9781139171731.009 Published online by Cambridge University Press

Fig. 8.1. Creep of a flexible belt transmitting a torque M between pulleys rotating at ω_1 and ω_2.

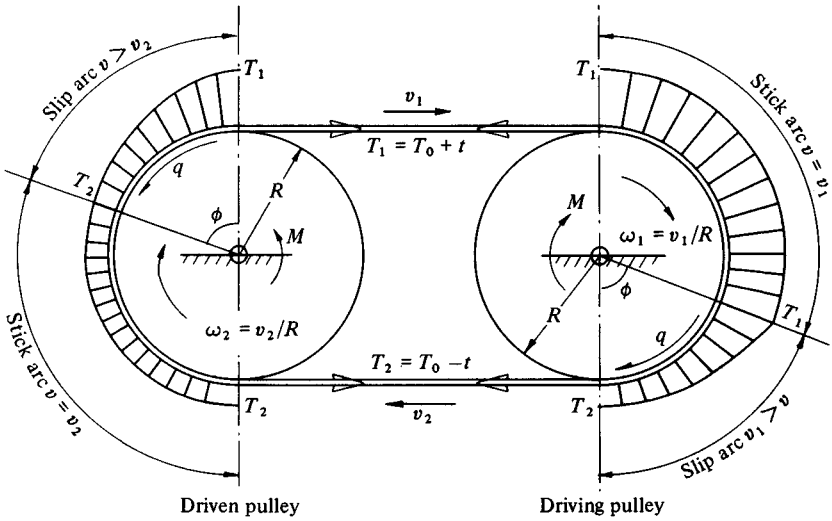

consistent with the general equation (8.1). Thus the velocity of the tight side v_1 is greater than that of the slack side v_2. We note that frictional traction q pulls the belt forward on the driving pulley, but drags it back on the driven pulley, as shown. Since friction must oppose the direction of slip (condition (8.7)) the pulley must be moving faster than the belt in the slip arc of the driver and slower than the belt in the slip arc of the driven pulley. The peripheral speed of the driving pulley must therefore be v_1, so that the stick arc is located where the belt runs onto the pulley. Similarly the peripheral speed of the driven pulley must coincide with v_2, whereupon the stick arc occurs at the run on to the driven pulley also. The creep ratio for the whole system may be defined by:

$$\xi \equiv \frac{(\omega_1 - \omega_2)R}{V} = \frac{v_1 - v_2}{V} = \lambda(T_1 - T_2) = \lambda M/R \tag{8.11}$$

Thus the driven pulley runs slightly slower than the driving pulley in proportion to the transmitted torque. The loss of power is expended in frictional dissipation in the slip arcs. The features exhibited by this one-dimensional example arise in the more complex cases now to be considered.

8.2 Freely rolling bodies having dissimilar elastic properties

Two elastic bodies which are geometrically identical and have the same elastic properties are completely symmetrical about their interface. When they roll freely under the action of a purely normal force, no tangential traction or

https://doi.org/10.1017/CBO9781139171731.009 Published online by Cambridge University Press

slip can occur, so that the contact stresses and deformation are given by the Hertz theory of static contact. In these circumstances the rolling process is completely reversible in the thermodynamic sense.

The problem of the stresses and micro-slip at the rolling contact of two bodies whose elastic constants differ, which was discussed qualitatively by Reynolds in 1875, has had to wait for nearly a century for a quantitative solution. The problem arises through a difference in the tangential strains in the two surfaces if the elastic constants of the bodies are different, which introduces tangential tractions and possible slip at the interface. This problem is the equivalent in rolling contact to the normal contact of dissimilar solids with friction discussed in §5.4.

(a) Freely rolling cylinders with parallel axes

The cylinders of radii R_1 and R_2 are pressed into contact by a force P per unit length which produces a contact area and contact pressure given by Hertz. In steady rolling it follows from condition (8.3) that the difference in tangential displacement gradients in a stick region is constant. Following the customary approach we shall assume first that friction is sufficient to prevent slip entirely, so that the strain difference is constant throughout the contact strip ($-a \leqslant x \leqslant a$). The strain $\partial \bar{u}_x/\partial x$ at each contact surface due to distributions of tangential and normal tractions $q(x)$ and $p(x)$ is given by equation (2.25*a*). When this expression is substituted into equation (8.3*a*), with the slip velocity $\dot{s}_x$ taken to be zero,

$$\pi\beta p(x) + \int_{-a}^{a} \frac{q(s)}{x-s}\,\mathrm{d}s = \tfrac{1}{2}\pi E^* \xi_x = \text{constant}, \quad -a \leqslant x \leqslant a \tag{8.12}$$

This equation and (5.27) comprise coupled integral equations for $p(x)$ and $q(x)$. They have been solved by Bufler (1959) using the method of §2.7 with class III boundary conditions. We shall simplify the problem by neglecting the effect of tangential traction on the normal pressure which is then given by Hertz. Equation (8.12) now provides a single integral equation for $q(x)$. Following the treatment of the static problem in §5.4, $q(x)$ is divided into two components $q'(x)$ and $q''(x)$. The traction $q'(x)$ is that necessary to eliminate the difference in strains due to the normal pressure; it is given by equation (5.32). $q''(x)$ is the traction required to give rise to a constant strain difference ξ_x; it is determined by an integral equation of the form specified in (2.39) and (2.44) where $n = 0$ and $A = \pi E^* \xi_x/2$ with the solution

$$q''(x) = \frac{E^* \xi_x}{2} \frac{x}{(a^2 - x^2)^{1/2}} \tag{8.13}$$

https://doi.org/10.1017/CBO9781139171731.009 Published online by Cambridge University Press

At the leading edge of a rolling contact the strain must be continuous as a material element proceeds from outside to inside. Hence q must be zero at the edge of contact. For this requirement to be satisfied the singular terms at $x = -a$ must vanish when $q'(x)$ and $q''(x)$ are added. This condition fixes the magnitude of the creep ratio to be

$$\xi_x = 4\beta p_0/\pi E^* = 2\beta a/\pi R \tag{8.14}$$

where $1/R = 1/R_1 + 1/R_2$, whereupon

$$q(x) = \frac{\beta}{\pi} p_0 (1 - x^2/a^2)^{1/2} \ln\left(\frac{a+x}{a-x}\right) \tag{8.15}$$

This traction is plotted in Fig. 8.2. For practical values of β (see Table 5.1) it is an order of magnitude smaller than the normal pressure and acts outwards on the more compliant surface and inwards on the more rigid one. Bufler's exact solution taking into account the influence of tangential traction on normal pressure gives results which differ only slightly from (8.14) and (8.15).

We now examine the possibility of slip. From equation (8.15) it is apparent that the ratio $q(x)/p(x)$ becomes infinite at $x = \pm a$, so that some slip is inevitable. To obtain an indication of the slip pattern it is instructive to

Fig. 8.2. Distributions of tangential traction in the rolling contact of dissimilar rollers ($\beta = 0.3$, $\mu = 0.1$). No slip: solid line – exact, Bufler (1959); chain line – approximate, eq. (8.15). Complete slip: broken line – $q(x) = \pm\mu p(x)$. Partial slip: line with spots – numerical solution, Bentall & Johnson (1967).

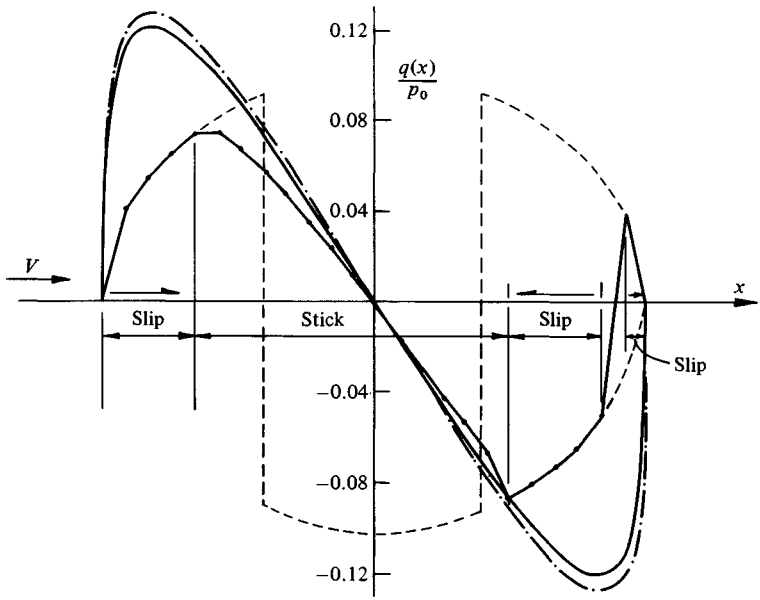

https://doi.org/10.1017/CBO9781139171731.009 Published online by Cambridge University Press

examine the other extreme case, in which the coefficient of friction is small, so that slip is unrestricted and the tangential traction is too small to affect the elastic deformation. The tangential strain in each surface is then given by the first term in equation (2.25*a*) where $p(x)$ is the Hertz pressure distribution. Substituting in (8.2) gives an expression for the slip velocity:

$$\frac{\dot{s}_x}{V} = \xi_x - (\beta a/4R)(1 - x^2/a^2)^{1/2} \tag{8.16}$$

If ξ_x has a suitable positive value the slip velocity, given by (8.16), is positive at the ends of the contact and negative in the centre. The frictional traction $\pm\mu p(x)$, though small, must change direction at two points symmetrically disposed about the origin. The location of these points, and hence the value of ξ_x, are determined by the condition that, in free rolling, the net tangential force is zero. This condition demands that the direction of slip reverses at $x = \pm 0.404a$ whereupon

$$\xi_x = 0.914\beta a/R \tag{8.17}$$

The true state of affairs must lie between the extremes of no-slip and complete slip. We might expect there to be two stick regions separating three regions in which there is slip in alternate directions. A numerical analysis by Bentall & Johnson (1967), using the method described in §5.9, has shown that this is the case. The solution is a function of the parameter (β/μ). The spread of the three micro-slip zones with increasing values of (β/μ) is shown in Fig. 8.3.

Fig. 8.3. Slip regions in the rolling contact of dissimilar rollers.

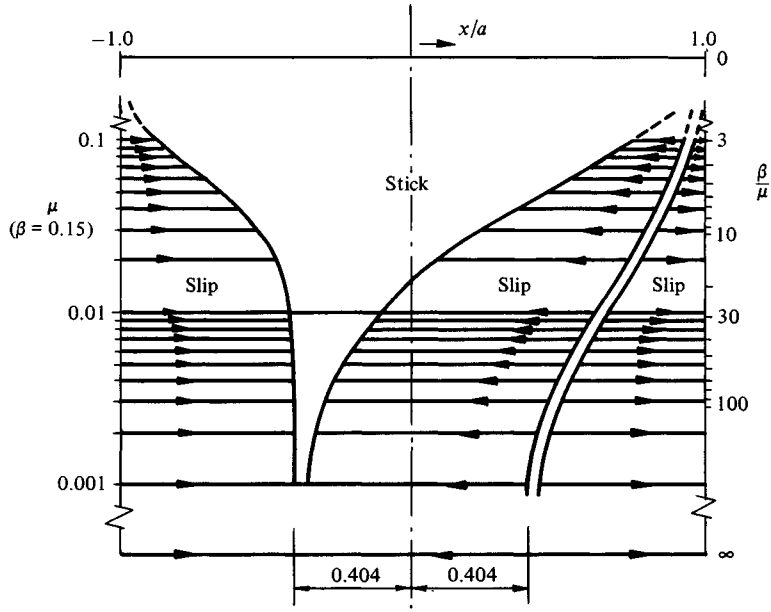

https://doi.org/10.1017/CBO9781139171731.009 Published online by Cambridge University Press

A typical distribution of tangential traction is shown in Fig. 8.2 where it is compared with the solutions for no-slip (equation (8.15)) and complete slip. It is interesting to note the rapid reversal of traction and slip direction experienced by contacting points as they pass towards the rear edge of the contact.

Rolling is no longer reversible; energy dissipation in the slip regions contributes to a moment M resisting rotation of the cylinders. This moment has been computed and is shown in Fig. 8.4.† As Reynolds predicted, the rolling resistance is low when μ is high, since micro-slip is prevented, and is again low when μ is small since the frictional forces are then small. Maximum resistance occurs at an intermediate value of $\mu \approx \beta/5$.

(b) Freely rolling spheres

Tractions at the interface of freely rolling dissimilar spheres can be approached along the same lines. We first assume no-slip and neglect the influence of tangential tractions on normal pressure. For no-slip, equations (8.3) require that the differences in displacement gradient $\{(\partial\bar{u}_{x1}/\partial x) - (\partial\bar{u}_{x2}/\partial x)\}$ and $\{(\partial\bar{u}_{y1}/\partial x) - (\partial\bar{u}_{y2}/\partial x)\}$ should be constant throughout the contact area and equal to $-\xi_x$ and $-\xi_y$ respectively. The tangential traction $q(x, y)$ which satisfies these conditions again may be divided into a component $q'(x, y)$ which eliminates the difference in tangential displacements due to normal pressure

† The tangential traction and slip, from which the dissipation has been calculated, have been found on the assumption that the pressure distribution is symmetrical and given by Hertz. In fact the asymmetry of the traction will give rise to a slight asymmetry in pressure which is responsible for the resisting moment.

Fig. 8.4. Rolling resistance of dissimilar rollers.

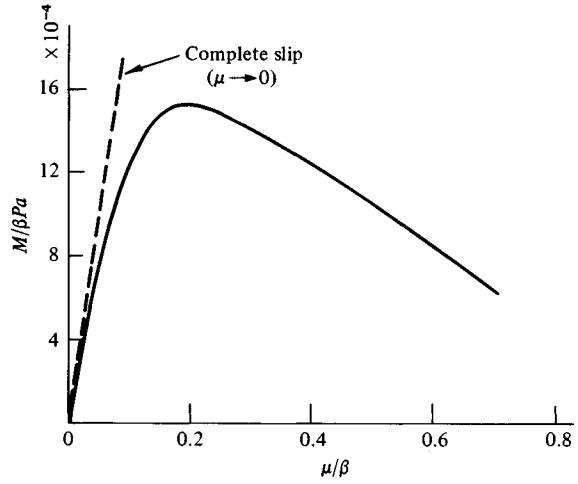

https://doi.org/10.1017/CBO9781139171731.009 Published online by Cambridge University Press

and a component $q''(x,y)$ which gives rise to the constant creep coefficients. The tangential displacements due to the Hertz pressure are radial and axi-symmetric: $q'(x,y)$ is therefore also radial and axi-symmetric ($=q'(r)$) and is given by equation (5.35). This traction contains a term $(a^2-r^2)^{-1/2}$ which must be annulled at the leading edge by an equal and opposite term in the expression for $q''(x,y)$. In order to satisfy the conditions of no-slip (eq. (8.3) and (8.4)) the resulting displacements within the contact area must satisfy the condition $\partial\bar{u}_y/\partial x = 0$. These conditions are satisfied by a state of uniform bi-axial strain: $\partial\bar{u}_x/\partial x = \partial\bar{u}_y/\partial y =$ constant. The traction which gives rise to this strain can be found by the method of §3.7 with the result

$$q''(r) = \frac{2E^*\xi_x}{\pi r}\{(a^2-r^2)^{1/2} - a^2(a^2-r^2)^{-1/2}\} \tag{8.18}$$

To remove the infinite traction at $r=a$ when $q''(r)$ is added to $q'(r)$ we take

$$\xi_x = \frac{\beta a}{\pi R} \tag{8.19}$$

whereupon

$$q(r) = \frac{\beta p_0}{\pi}\left\{-\frac{a}{r}(a^2-r^2)^{1/2} + \frac{1}{r}\int_r^a \frac{t^2}{(t^2-r^2)^{1/2}}\ln\left(\frac{t+r}{t-r}\right)\mathrm{d}t\right\} \tag{8.20}$$

An exact solution to this problem has been obtained by Spence (1968).

In common with the two-dimensional case there must be some slip at the edge of the contact circle but once slip has occurred the traction is no longer axi-symmetric and no solution is at present available.

Equation (8.19) has been checked by experiments in which the distance rolled by a ball in one revolution has been accurately measured and compared with the undeformed circumference of the ball. Measurements (*a*) with a Duralumin ball rolling between two parallel steel planes and (*b*) a steel ball between Duralumin planes ($\beta = \pm 0.12$) are shown in Fig. 8.5. The average of these two experiments agrees well with equation (8.19) for the creep calculated by neglecting slip. The small difference between the two experiments is due to various second-order effects: (i) points on the periphery of the ball lie at different radii from the axis of rotation. This effect, frequently referred to as 'Heathcote slip', is considered in §5. For a ball on a plane a creep ratio $\xi_x = -0.125(a/R)^2$ is predicted. (ii) the interface is curved such that the surface of the ball is compressed and that of the plane is stretched by an amount of order $\xi_x = -0.10(a/R)^2$. These estimates are consistent in sign and order of magnitude with the discrepancy between the creep measurements and equation (8.19) but they are hardly significant in comparison with the second-order errors introduced by the linear theory of elasticity.

https://doi.org/10.1017/CBO9781139171731.009 Published online by Cambridge University Press

Fig. 8.5. Free rolling creep of a ball on a plane of dissimilar material. Cross – Duralumin ball on steel plane; circle – steel ball on Duralumin plane; broken line – average experimental line; chain line – theory, eq. (8.19).

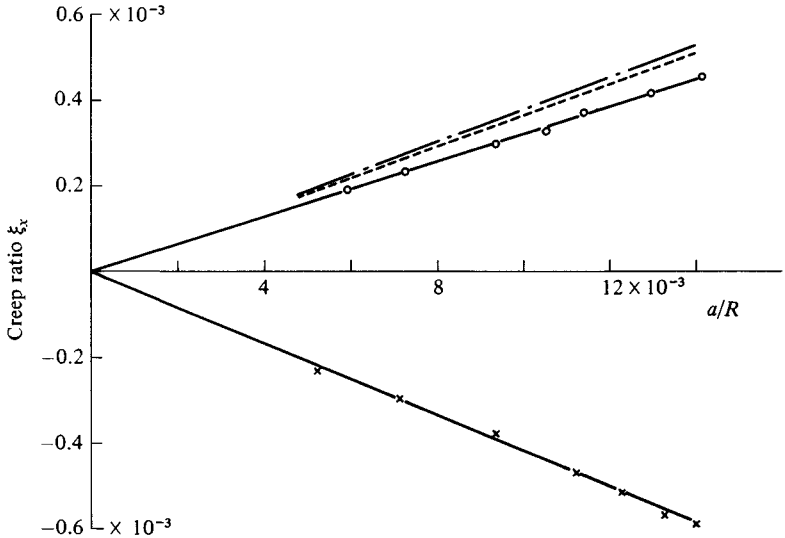

8.3 Tractive rolling of elastic cylinders

In this section we consider rolling cylinders which transmit a resultant tangential (tractive) force through friction at the interface, such as the wheel of a vehicle which is driving or braked. To eliminate the effects discussed in the last section we shall consider elastically similar cylinders. The first solution to this problem in its two-dimensional (plane strain) form was presented by Carter (1926) and independently by Fromm (1927), Föeppl (1947), Chartet (1947) and Poritsky (1950).

From our discussion of two stationary cylinders which transmit a tangential force less than limiting friction (§7.2), we would expect the contact area to be divided into zones of slip and stick. It is instructive to start by examining the solution to the static problem in light of the conditions of stick and slip in rolling contact established in §1 of this chapter. In the static case (Fig. 7.7) there is a central stick region in which tangential displacement is constant, with equal regions of micro-slip on either side. The strains in the stick region ($\partial \bar{u}_x/\partial x = 0$) satisfy condition (8.4) for no slip in rolling contact, and the tractions shown in Fig. 7.7 satisfy conditions (8.5) and (8.6). However, condition (8.7), which requires the direction of slip to oppose the traction in a slip zone, is violated in the slip zone at the leading edge of the contact.

https://doi.org/10.1017/CBO9781139171731.009 Published online by Cambridge University Press

This result leads us to expect the stick region to be located adjacent to the leading edge of the contact area and for slip to be confined to a single zone at the trailing edge. The same conclusion was reached in the one-dimensional example of a belt being driven on a pulley.

The distribution of tangential traction in the static case comprises the superposition of two elliptical distributions $q'_x(x)$ and $q''_x(x)$ given by equations (7.23) and (7.25) respectively. The traction $q'_x(x)(=\mu p_0(1-x^2/a^2)^{1/2})$ produces a tangential strain within the contact strip, by equation (7.24),

$$\frac{\partial \bar{u}'_x}{\partial x} = -\frac{2(1-\nu^2)}{aE}\mu p_0 x \tag{8.21}$$

We displace the centre of $q''(x)$ by a distance $d\,(=a-c)$ so that it is now adjacent to the leading edge, as shown in Fig. 8.6.

$$q''_x(x) = -\frac{c}{a}\mu p_0\{1-(x+d)^2/c^2\}^{1/2} \tag{8.22}$$

Within the strip $(-a \leqslant x \leqslant c-d)$ it produces a tangential strain:

$$\frac{\partial \bar{u}''_x}{\partial x} = \frac{c}{a}\frac{2(1-\nu^2)}{cE}\mu p_0(x+d) \tag{8.23}$$

Adding (8.23) to (8.21) gives the resultant tangential strain in the strip $(-a \leqslant x \leqslant c-d)$ to be

$$\frac{\partial \bar{u}_x}{\partial x} = \frac{2(1-\nu^2)}{aE}\mu p_0 d = \text{constant}$$

The tractions acting on each surface are equal and opposite so that the tangential strains in each surface are equal and of opposite sign. Thus substituting in equation (8.3), we see that the condition of no-slip (8.4) is satisfied in the strip $(-a \leqslant x \leqslant a-d)$ with the creep ratio given by:

$$\xi_x = -4(1-\nu^2)\mu p_0 d/aE \tag{8.24}$$

The resultant traction $q_x(x) = q'_x(x) + q''_x(x)$ satisfies the conditions (8.5) and (8.6) in both slip and stick zones, and the direction of slip satisfies (8.7). As in the static case (eq. 7.29), the width of the stick region is determined by the magnitude of the tangential force, whence

$$\frac{d}{a} = 1 - \frac{c}{a} = 1 - (1 - Q_x/\mu P)^{1/2} \tag{8.25}$$

whereupon, by using the Hertz relationship for p_0, the creep ratio is given by

$$\xi_x = -\frac{\mu a}{R}\{1-(1-Q_x/\mu P)^{1/2}\} \tag{8.26}$$

https://doi.org/10.1017/CBO9781139171731.009 Published online by Cambridge University Press

where $1/R = 1/R_1 + 1/R_2$. The relationship between ξ_x and Q_x, plotted in Fig. 8.7, is known as a 'creep curve'.

The action of a tractive force, however small, causes some micro-slip at the trailing edge of the interface. The slip region spreads forwards with increasing tangential force until, when $Q = \mu P$, the slip zone reaches the leading edge and complete sliding occurs.

Fig. 8.6. Tractive rolling contact of similar cylinders; (*a*) distribution of tangential tractions - chain line - no slip, eq. (8.27); (*b*) surface strains $\partial u_x/\partial x$.

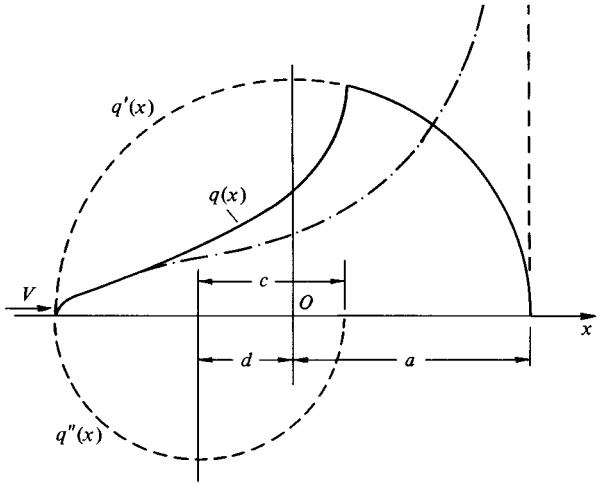

(*a*)

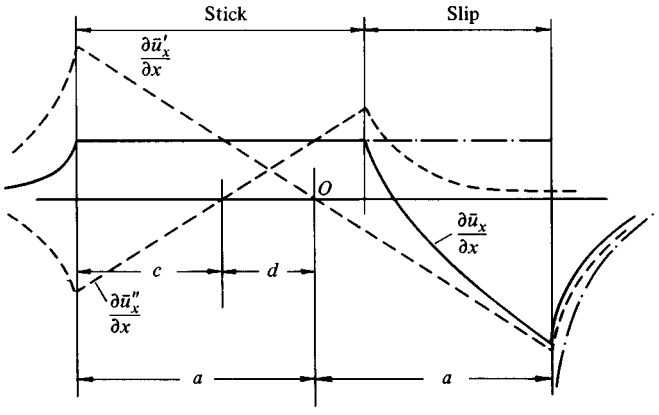

(*b*)

https://doi.org/10.1017/CBO9781139171731.009 Published online by Cambridge University Press

The state of stress in the cylinders due to a traction of the form $q'(x)$ has been discussed in §7.1. The stresses in the rolling contact case can be found by superposition of $q'_x(x)$ and $q''_x(x)$ (see §9.2).

Under conditions of high friction, such that $Q/\mu P$ is small, the slip region at the trailing edge becomes vanishingly small and the distribution of tangential traction approaches the limiting form:

$$q_x(x) = \frac{p_0}{2} \frac{a+x}{(a^2-x^2)^{1/2}} \frac{Q_x}{P} \tag{8.27}$$

The corresponding limit for the creep ratio is

$$\xi_x = aQ_x/2RP \tag{8.28}$$

This relationship corresponds to a linear creep curve (Fig. 8.7), whose gradient is referred to as the *creep coefficient.* The traction of (8.27) is zero at the leading edge; in consequence the strain is continuous from outside to inside the contact boundary, as can be seen from Fig. 8.6(*b*). At the trailing edge there is a singularity in traction just inside the contact and a singularity in strain just outside. In reality the singularities will be relieved by slip but we can think of it as a limit in which the elastic strain energy built up through the contact is dissipated instantaneously and irreversibly at the trailing edge. The rate of energy so dissipated is given by the product of the tractive force and the creep ratio, i.e.

$$\dot{W} = Q_x \xi_x V = aQ_x^2 V/2RP \tag{8.29}$$

Fig. 8.7. Creep curve for tractive rolling contact of cylinders. Solid line – Carter's (1926) creep curve, eq. (8.26); broken line – no slip, eq. (8.28); chain line – elastic foundation, eq. (8.69).

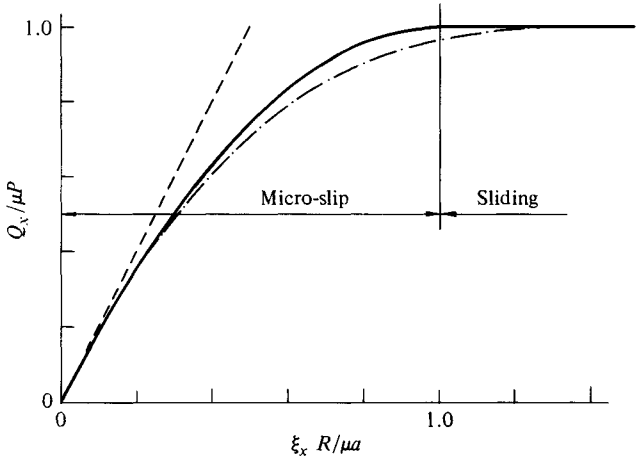

https://doi.org/10.1017/CBO9781139171731.009 Published online by Cambridge University Press

The results obtained in this section strictly apply only when the two cylinders are elastically similar, otherwise additional tangential tractions are present as discussed in the previous section. Under high friction conditions (small regions of micro-slip) the results of the two sections can be superposed. Generally the influence of the tractive force outweighs that of the difference in elastic constants whereupon the above results can be used with $E/(1-\nu^2)$ replaced by $2E^*$. Interaction between the two effects has been analysed numerically by Kalker (1971*a*).

When a tangential force Q_y acts parallel to the axis of the cylinders tangential tractions and micro-slip arise in the axial direction. The surface displacements and internal stresses produced by the distribution of tangential traction

$$q_y'(x) = \mu p_0 (1 - x^2/a^2)^{1/2}$$

have been found in §2.9. The surface displacement gradients for $(-a \leqslant x \leqslant a)$ are

$$\frac{\partial \bar{u}_x}{\partial x} = 0, \quad \frac{\partial \bar{u}_y}{\partial x} = -\frac{\mu p_0}{G}\frac{x}{a} \tag{8.30}$$

This relationship is similar to that expressed by equation (8.21) except for the change in elastic constant from $(1-\nu^2)/E$ to $(1/2\pi G)$. The analysis of the present case is, therefore, completely analogous to that for a longitudinal tangential force. The contact region is divided into a stick region at the leading edge and slip region at the trailing edge. The axial traction is found by the superposition of q_y' and $q_y''(= -q_x' c/a)$ as before, where the extent of the slip region is given by (8.25). The axial creep ratio is given by substituting equation (8.30) for each surface in (8.3*b*) with the result:

$$\xi_y = -\left(\frac{1}{G_1} + \frac{1}{G_2}\right)\mu p_0 \{1 - (1 - Q_y/\mu P)^{1/2}\} \tag{8.31}$$

Cases of combined axial and longitudinal traction have been examined by Heinrich & Desoyer (1967) and Kalker (1967*a*).

8.4 Rolling with traction and spin of three-dimensional bodies

Three-dimensional bodies in rolling contact may be called upon to transmit tangential forces, Q_x in the longitudinal and Q_y in the transverse directions, while being subjected to a relative angular velocity about the normal axis $(\Delta\omega_z \equiv \omega_{z1} - \omega_{z2})$ referred to as spin. The spin motion tends to twist the contact interface and hence also gives rise to tangential tractions and micro-slip. In the two-dimensional situations considered previously stick and slip zones comprised strips parallel to the y-axis. The three-dimensional case is much more complex. Contact is made on an elliptical area; the shape of the

https://doi.org/10.1017/CBO9781139171731.009 Published online by Cambridge University Press

stick and slip zones are not known *a priori* and condition (8.7), which requires the tangential traction in a slip zone to oppose the relative slip, couples the effects of tangential forces and spin in a nonlinear manner.

In face of the difficulty caused by the unknown pattern of stick and slip, we will consider first the situation where the coefficient of friction is sufficiently great to prevent slip and take a lead from the two-dimensional case analysed in §3.

(a) Vanishing slip ($\mu \to \infty$): linear creep theory

If the coefficient of friction is sufficiently high, slip is limited to a vanishingly thin zone at the trailing edge of the contact. In this case we seek tangential tractions which satisfy the no-slip conditions (8.3), (8.4) and (8.5) throughout the contact area. For simplicity we shall begin with a circular contact subjected to a longitudinal tangential force Q_x which is the three-dimensional equivalent of the situation examined in the previous section. On the basis of the two-dimensional case (eq. (8.27)), we consider the traction

$$q_x(x,y) = \frac{Q_x}{2\pi a^2} \frac{a+x}{(a^2-r^2)^{1/2}} \tag{8.32}$$

The tangential displacements within the contact circle ($r \leqslant a$) produced by this traction may be found by substitution in equation (3.83*a* and *b*) and by performing the integrations, with the result:

$$\frac{\partial \bar{u}_x}{\partial x} = \frac{Q_x(4-3\nu)}{32Ga^2} \; ; \quad \frac{\partial \bar{u}_y}{\partial x} = 0 \tag{8.33}$$

These displacement gradients are constant throughout the contact region and hence satisfy the conditions of no-slip (8.3) and (8.4), with creep ratios:

$$\xi_x = -\frac{(4-3\nu)}{16Ga^2} Q_x; \quad \xi_y = 0 \tag{8.34}$$

Under the action of a transverse tangential force Q_y, the traction

$$q_y(x,y) = \frac{Q_y}{2\pi a^2} \frac{a+x}{(a^2-r^2)^{1/2}} \tag{8.35}$$

satisfies the conditions of no-slip and results in a transverse creep:

$$\xi_y = -\frac{(4-\nu)Q_y}{16Ga^2} \; ; \quad \xi_x = 0 \tag{8.36}$$

Due to the asymmetry of the traction distribution (8.35) it exerts a twisting moment about O given by

$$M_z = -\tfrac{1}{3} Q_y a = \{16/3(4-\nu)\}\xi_y$$

https://doi.org/10.1017/CBO9781139171731.009 Published online by Cambridge University Press

In the case of pure spin, distributions of traction can be found (Johnson, 1958*b*) which satisfy the conditions of no-slip, viz.:

$$q_x = \frac{8G(3-\nu)}{3\pi(3-2\nu)}\psi\frac{(a+x)y/a}{(a^2-r^2)^{1/2}} \tag{8.37a}$$

and

$$q_y = \frac{8G(1-\nu)}{3\pi(3-2\nu)}\psi\frac{(a^2-2x^2-ax-y^2)/a}{(a^2-r^2)^{1/2}} \tag{8.37b}$$

where ψ is the spin parameter defined on p. 244. These tractions correspond to zero resultant force ($Q_x = Q_y = 0$) but give rise to a resultant twisting moment M_z, which resists the spin motion, given by:

$$M_z = \frac{32(2-\nu)}{9(3-2\nu)}Ga^3\psi \tag{8.38}$$

When the displacement gradients due to the tractions of (8.37) are substituted into the conditions of no-slip (8.3) and (8.4), the creep ratios are found to be:

$$\xi_x = 0; \quad \xi_y = \frac{2(2-\nu)}{3(3-2\nu)}\psi \tag{8.39}$$

It is perhaps surprising at first sight that pure spin gives rise to transverse creep, but this phenomenon has been well supported by experiment. For details of the above analysis see Johnson (1958*a* & *b*).

The tentative distributions of traction for rolling with traction and spin proposed in equations (8.32), (8.35) and (8.37) do not satisfy the no-slip conditions completely. To do so they must vanish at all points on the leading edge of the contact. We see that, in each case, $q = 0$ at the 'leading point' $(-a, 0)$, but that elsewhere along the leading edge q is unbounded.

To overcome this difficulty Kalker (1964, 1967*a*) made use of the fact (see §3.7(*e*)) that a general traction:

$$q(x,y) = A_{mn}(x/a)^m(y/b)^n\{1-(x/a)^2-(y/b)^2\}^{-1/2} \tag{8.40}$$

gives rise to tangential displacements $\bar{u}_x$ and $\bar{u}_y$ each of which varies throughout the elliptical contact region as a polynomial in x and y of order $(m+n)$. By appropriate superposition of tractions of the form (8.40) the displacement gradients can be made to satisfy the condition of no-slip throughout the contact ellipse, while maintaining a zero value of q along the leading edge. In carrying out the necessary computations Kalker truncated the series at $m+n=5$ and minimised the integrated traction round the leading edge, which amounted to making $q = 0$ at a finite number of points on the leading edge. From this point of view the results expressed above in equations (8.32)–(8.38) may be regarded as the first approximation to Kalker's solution, taking $m+n=2$ and satisfying the condition $q = 0$ at one point $(-a, 0)$ only.

Since this is a linear theory there is no interaction between longitudinal and transverse forces and the effects can be superposed. The results may conveniently be summarised in three linear creep equations:

$$\frac{Q_x}{Gab} = C_{11}\xi_x \tag{8.41}$$

$$\frac{Q_y}{Gab} = C_{22}\xi_y + C_{23}\psi \tag{8.42}$$

$$\frac{M_z}{G(ab)^{3/2}} = C_{32}\xi_y + C_{33}\psi \tag{8.43}$$

where C_{11}, C_{22} etc. are non-dimensional creep coefficients found from the theory.

A shortened table of the creep coefficients found by Kalker (1967*a*) for elliptical contact areas of varying eccentricity is given in Appendix 4. The approximate values for a circular area obtained from equations (8.34), (8.36) and (8.38) are given for comparison.

(b) Complete slip

At the other extreme, when the creep and spin ratios become large and the coefficient of friction is small, the elastic deformation due to the tangential tractions becomes small. In the expressions for slip velocities (8.3) the elastic displacement terms can be neglected, so that slip vanishes at one point $P(x_p, y_p)$ only (see Fig. 8.8), where

$$x_p/a = -\xi_y/\psi \quad \text{and} \quad y_p/a = \xi_x/\psi \tag{8.44}$$

Fig. 8.8. Rolling with creep and spin: location of the 'spin pole', *P*.

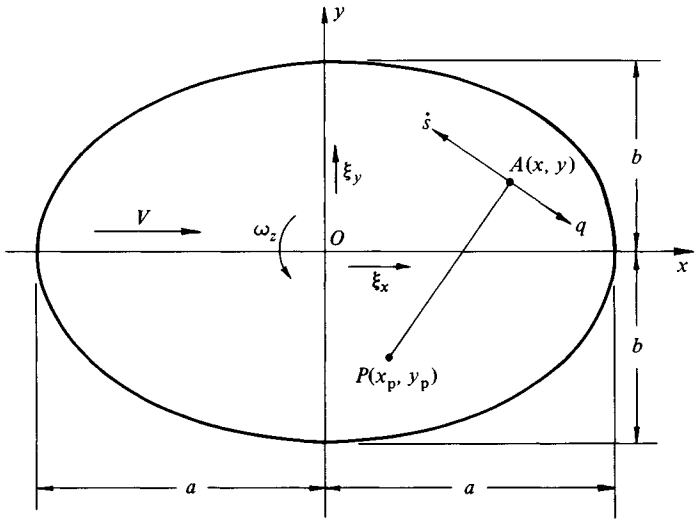

https://doi.org/10.1017/CBO9781139171731.009 Published online by Cambridge University Press

This point is known as the *spin pole*; it may lie inside or outside the contact area. Since elastic deformation in the x-y plane is neglected, the relative motion of the surfaces comprises a rigid rotation with angular velocity $(\omega_{z1} - \omega_{z2})$ about the spin pole. At any point $A(x, y)$ the resultant tangential traction $q(x, y)$ has the magnitude $\mu p(x, y)$ in the direction perpendicular to the line PA. The forces Q_x, Q_y and the moment M_z corresponding to any combination of creep and spin can be readily computed by numerical integration. Such computations have been carried out for circular contacts by Lutz (1955 *et seqq.*) and for elliptical contacts by Wernitz (1958) and Kalker (1967*a*). The influence of spin upon the creep curves under the action of tangential tractions, calculated on the basis of complete slip, is shown in Fig. 8.11. The interaction between spin and traction plays an important role in the operation of rolling contact friction drives.

(c) Partial slip: nonlinear creep theory

The distributions of traction calculated on the assumption of no slip are zero at the leading edge and rise progressively through the contact area to infinite values at the trailing edge. We would, therefore, expect slip to start at the trailing edge and to spread forward through the contact area with an increase in the tractive forces as in the two-dimensional contact analysed in §3. This conjecture is borne out by experiment. Observations by Ollerton & Haines (1963) of the contact ellipse between photo-elastic models show the stick region to be roughly 'lemon' shaped. One edge coincides with the leading edge of the contact ellipse and the boundary with the slip zone is a reflection of the leading edge. Experiments using a rubber ball rolling with spin on a transparent plane (Johnson, 1962*a*) revealed the stick zone to be 'pear' shaped with one boundary coincident with the leading edge of the contact circle. When stick and slip zones coexist in the contact area the distribution of traction and equations for creep have, so far, been found only approximately. Three methods have been tried.

In the first method, the stick zone under the action of a tangential force (without spin) is assumed to be an ellipse, similar to the contact ellipse, and touching it at the leading point $(-a, 0)$ shown in Fig. 8.9. This assumption has the merit of giving simple expressions in closed form for the traction and creep (Johnson, 1958*a*, *b*; Vermeulen & Johnson, 1964). For a circular contact area, transmitting Q_x alone, the creep is given by

$$\xi_x = -\frac{3\mu P(4-3\nu)}{16Ga^2}\left\{1-\left(1-\frac{Q_x}{\mu P}\right)^{1/3}\right\} \tag{8.45}$$

and when transmitting Q_y alone

https://doi.org/10.1017/CBO9781139171731.009 Published online by Cambridge University Press

$$\xi_y = -\frac{3\mu P(4-\nu)}{16Ga^2}\left\{1-\left(1-\frac{Q_x}{\mu P}\right)^{1/3}\right\} \tag{8.46}$$

When $Q \ll \mu P$ these equations reduce to the linear creep equations (8.34) and (8.36) which neglect slip. The assumption of an elliptical stick region is clearly in error since it does not include the leading edge of the contact circle.

This particular difficulty is avoided by a quite different approach to the problem suggested by Haines & Ollerton (1963) and developed by Kalker (1967*b*). In their method the contact area is divided into thin strips parallel

Fig. 8.9. Tractive rolling of an elliptical contact region under a longitudinal force Q_x. Broken line – elliptical stick zone, Johnson (1958*a*); chain line – strip theory, Haines & Ollerton (1963).

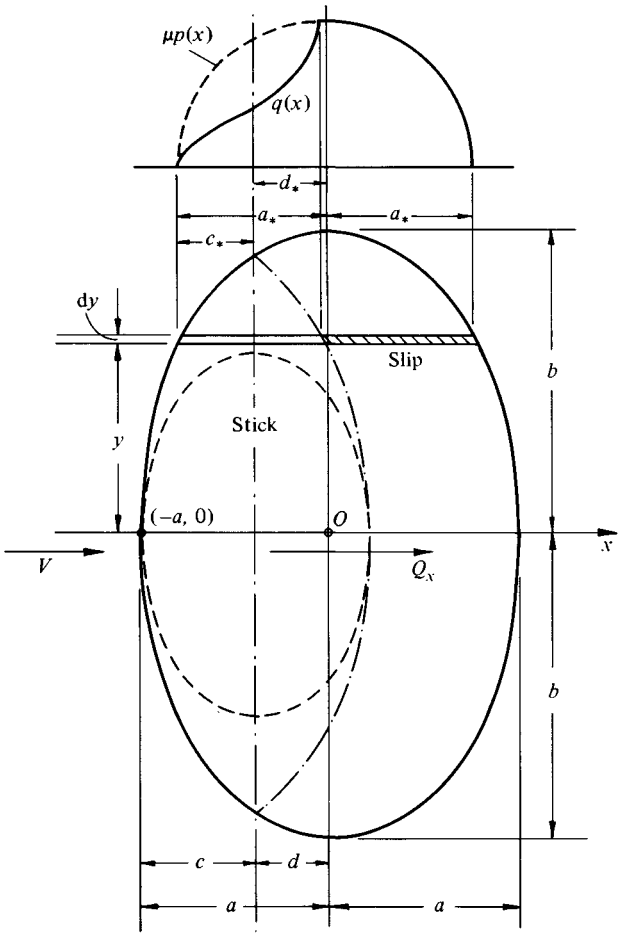

https://doi.org/10.1017/CBO9781139171731.009 Published online by Cambridge University Press

to the rolling direction (x-axis). The two-dimensional theory from §3 above is then applied to each strip, neglecting interaction between adjacent strips. We shall apply their method to an elliptical contact under the action of a longitudinal tangential force Q_x only (see Fig. 8.9).

A typical strip, distance y from the x-axis has a length $2a_*$ and supports a pressure

$$p(x) = p_0^*(a_*^2 - x^2)^{1/2}$$

where

$$\frac{p_0^*}{p_0} = \frac{a_*}{a} = (1 - y^2/b^2)^{1/2} \tag{8.47}$$

We now assume that Carter's theory for cylindrical contact can be applied to the strip. A stick region of length $2c_*$ is located adjacent to the leading edge. The creep ratio is given by equation (8.24), with p_0, d and a replaced by p_0^*, d_* and a_* respectively, whence

$$\xi_x = -\frac{2(1-\nu)}{Ga_*}\mu p_0^* d_* \tag{8.48}$$

Now the creep ratio ξ_x must be a constant for the contact as a whole, hence it follows from equation (8.48) that $d_*(=a_* - c_*)$ has the same value for all the strips in which a stick zone exists. Thus the mid-points of the stick zones lie on the straight line $x = -d_*$. The curve separating the stick and slip zones is therefore a reflexion of the leading edge in this line, giving rise to a lemon shaped stick zone as observed experimentally.

The distribution of traction on a strip follows Carter and is shown in Fig. 8.9. The tangential force $\mathrm{d}Q_x$ provided by a strip is determined by equation (8.25) i.e.

$$\mathrm{d}Q_x = \mu P_*(1 - c_*^2/a_*^2)\,\mathrm{d}y$$

$$= \frac{\pi}{2}\mu p_0 a(1 - y^2/a^2)\{1 - (1 - d_*/a_*)^2\}\,\mathrm{d}y$$

The total force Q_x is found by integration of equation (8.49) over the contact area, noting that, when $y > a^2 - d_*^2$, the stick region vanishes so that the term $(1 - d_*/a_*)$ is put equal to zero, with the result:

$$Q_x/\mu P = \tfrac{3}{2}\zeta_x \cos^{-1}(\zeta_x) + \{1 - (1 + \tfrac{1}{2}\zeta_x^2)(1 - \zeta_x^2)^{1/2}\} \tag{8.49}$$

where $\zeta_x = \xi_x G/\mu p_0$. For vanishingly small slip ($\mu \to \infty$) this expression becomes

$$Q_x = \frac{\pi^2}{4}\frac{Gab}{1-\nu}\xi_x \tag{8.50}$$

The value of the creep coefficient given by the strip theory (8.50) is independent of the shape of the contact ellipse. It is compared with Kalker's value for

https://doi.org/10.1017/CBO9781139171731.009 Published online by Cambridge University Press

vanishingly small slip in Appendix 5. As might be expected the agreement is good when the ellipse is thin in the rolling direction ($b \gg a$), but the effect of neglecting interaction between the strips becomes serious for contacts in which $b < a$.

To apply the strip theory to contacts transmitting a transverse force Q_y or rolling with spin, use is made of the two-dimensional theory of transverse traction given in §2.9. For further details the reader is referred to Kalker (1967*b*). It is clear, however, that the strip theory is not satisfactory unless $b > a$; it breaks down completely when the spin motion is large. For these circumstances Kalker (1967*a*) devised a different approach based upon numerical techniques of optimisation.

The difficulty of problems involving micro-slip lies in the different boundary conditions which have to be satisfied for the stick and slip zones when the configuration of these zones is not known in advance. Kalker's approach to this difficulty is to combine the separate conditions of stick and slip into a single condition which is satisfied approximately throughout the contact area. If the tangential traction is denoted by the vector $\mathbf{q}$ and the slip velocity by the vector $\dot{\mathbf{s}}$, then we may combine the conditions of (8.4)–(8.7) in the statements

$$|\dot{\mathbf{s}}|\mathbf{q} + \mu p \dot{\mathbf{s}} = 0 \tag{8.51}$$

and

$$|\mathbf{q}| \leqslant \mu p \tag{8.52}$$

In a stick region $\dot{\mathbf{s}} = 0$ so that (8.51) is automatically satisfied; in a slip region $|\mathbf{q}| = \mu p$ in the opposite direction to $\dot{\mathbf{s}}$, so that (8.51) is again satisfied. Thus the correct distributions of slip and traction satisfy equations (8.51) and (8.52) throughout the whole contact area. A measure of the closeness with which any proposed distribution of traction satisfies the boundary conditions may be obtained by forming the integral over the contact area

$$I = \int_A (|\dot{\mathbf{s}}|\mathbf{q} + \mu p \dot{\mathbf{s}})^2 \, \mathrm{d}A \tag{8.53}$$

Since the integral is positive everywhere and zero when the boundary conditions are satisfied, the value of I is always positive and approaches zero when the correct distribution of traction and corresponding slip are inserted. Thus, out of any class of traction distributions, the 'best fit' is that which minimises I. Well developed techniques of nonlinear programming are available to assist in performing this minimisation.

This approach, unlike those discussed previously, blurs the distinction between stick and slip zones, which are now identified *a posteriori*: where $|\dot{\mathbf{s}}| \cong 0$ is identified as a stick zone; where $|q| \approx \mu p$ is identified as a slip zone.

https://doi.org/10.1017/CBO9781139171731.009 Published online by Cambridge University Press

Approximate distributions of traction may be found by the superposition of distributions of the form expressed in equation (8.40). Alternatively they may be made up of discrete traction elements in the manner described in §5.9. The tangential displacements $\bar{u}_x$ and $\bar{u}_y$ are calculated by the methods of §3.6 and substituted in equations (8.3) for the slip velocity $\dot{s}$. The optimum distribution of traction is then found from the minimisation of the integral I of (8.53).† Values of Q_x, Q_y and M_z have been calculated for various combinations of creep and spin ξ_x, ξ_y and ψ with elliptical contacts of varying eccentricity. (See Kalker (1969) for a summary of results.)

Creep forces play an important role in the guidance and stable running of railway vehicles. They arise as shown in Fig. 8.10. The point of contact is taken to be at rest, so that the rail moves relative to it with the forward speed of the vehicle V_1. The wheel profiles are coned so that longitudinal creep ξ_x can arise when the two wheels of a pair are running on different radii. Longitudinal creep is also a consequence of driving or braking a wheel. Lateral creep ξ_y arises if, during forward motion of the wheelset, the plane of the wheel is

Fig. 8.10. Creep motion of a railway wheel. Longitudinal creep ratio: $\xi_x = (V_2 - V_1)/V_1$; lateral creep ratio: $\xi_y = \delta V_y/V_1 = \tan \phi$; spin parameter: $\psi = \omega(ab)^{1/2}/V_1 = \{(ab)^{1/2}/R\} \tan \lambda$.

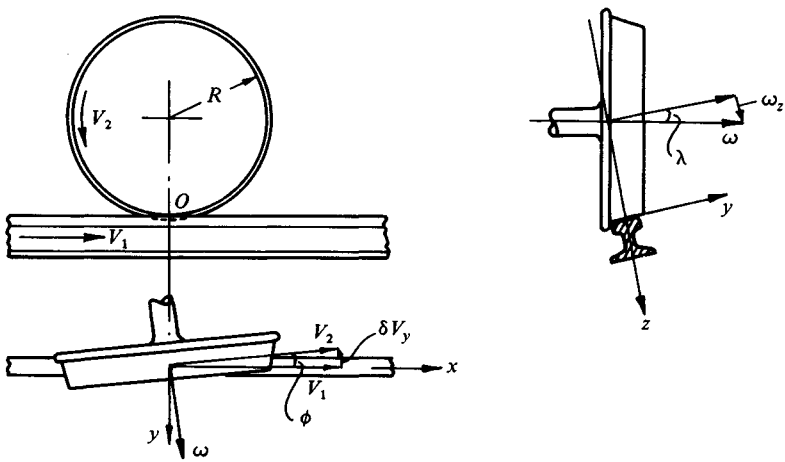

† More recently on grounds of versatility and dependability Kalker (1979) has abandoned the object function in the integral of equation (8.46) in favour of the complementary energy principle of Duvaut & Lions (1972) discussed in §5.9. In this approach the Eulerian formulation in §1 of this chapter is replaced by a Lagrangian system in which the moving contact area is followed and the traction is built up incrementally with time from some initial state until a steady state is approached. Such transient behaviour is discussed further in §6.

skewed through a small angle ϕ to the axis of the rail. Finally, since the common normal at the point of contact is tilted at the cone angle λ to the axis of rotation, the wheel has an angular velocity of spin $\omega_z = \omega \sin \lambda$ relative to the rail. For sufficiently small values of creep and spin the linear theory, embodied in equations (8.41)-(8.43), is adequate to determine the creep forces. At larger values the nonlinear theory, involving partial slip, must be used. For large creep and spin the creep forces are said to 'saturate' and their values are given by the 'complete slip' theory which does not depend upon elastic deformation tangential to the surface.

We shall conclude this section with an assessment of creep theory in relation to experimental observations. Surface tractions and associated internal stresses have been investigated by photo-elasticity using large epoxy-resin models in very slow rolling (Haines & Ollerton, 1963; Haines, 1964-5). The stick and slip zones were clearly visible. In the slip zone the traction closely follows Amonton's Law of friction as assumed in the theory. The measured traction in a circular contact transmitting a longitudinal force is compared with Carter's distribution (strip theory) and with Kalker's (1967*a*) continuous distribution in Fig. 8.11. The measured traction is very close in form to Carter's distribution, but the strip theory gives rise to an error in the size of the stick region. Kalker's method removes the sharp distinction between stick and slip, but in view of the small number of terms employed gives a remarkably good approximation to the measured traction.

Fig. 8.11. Tangential traction $q(x)$ on centre-line of circular contact transmitting a longitudinal force $Q_x = 0.72\mu P$. Solid line - numerical theory, Kalker (1967*a*); chain line - strip theory; circle - photo-elastic measurements.

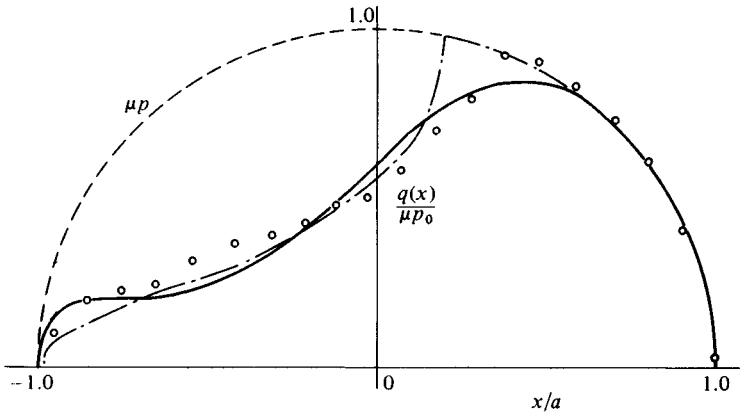

https://doi.org/10.1017/CBO9781139171731.009 Published online by Cambridge University Press

Creep experiments are usually performed by accurately measuring the distance traversed by a rolling element in precisely one revolution. Laboratory experiments by Johnson (1958*a* & *b*, 1959) in slow rolling using good quality surfaces are generally in good accord with present theory. The case of longitudinal creep is illustrated in Fig. 8.12 for a circular contact (a ball rolling on a plane). The influence of spin is governed by the non-dimensional parameter $\chi = \psi\bar{R}/\mu c$, where

$$1/\bar{R} = \tfrac{1}{4}\{(1/R_1') + (1/R_1'') + (1/R_2') + (1/R_2'')\} \quad \text{and} \quad c = (ab)^{1/2}$$

For a ball of radius R rolling on a plane, $\bar{R} = 2R$ and $c = a$. It is clear that increasing spin has the effect of reducing the gradient of the linear part of the creep curve, i.e. reducing the creep coefficient. The full lines denote Kalker's numerical nonlinear theory, which is well supported by the experiments. For no spin ($\chi = 0$), chain and dotted lines represent respectively the strip theory (eq. (8.49)) and Johnson's approximate theory (eq. (8.45)). The discrepancies, of opposite sign in each case, are not large, particularly in view of the practical uncertainty in the value of μ. Provided that the traction force Q_x is less than about 50% of its limiting value ($Q_x/\mu P < 0.5$), the linear theory, which assumes vanishingly small slip, provides a reasonable approximation. The predictions of Wernitz' complete slip theory, which neglect the tangential elastic compliance of the rolling bodies, have been added by the broken lines in Fig. 8.12. When there is no spin ($\chi = 0$) this theory is entirely inadequate since it

Fig. 8.12. Longitudinal creep combined with spin: theories and experiment (circular contact). Solid line – numerical theory, Kalker (1967*a*); large-dashed line – complete slip theory, Wernitz (1958); small-dashed line – approximate theory, eq. (8.45); chain line – strip , theory eq. (8.49).

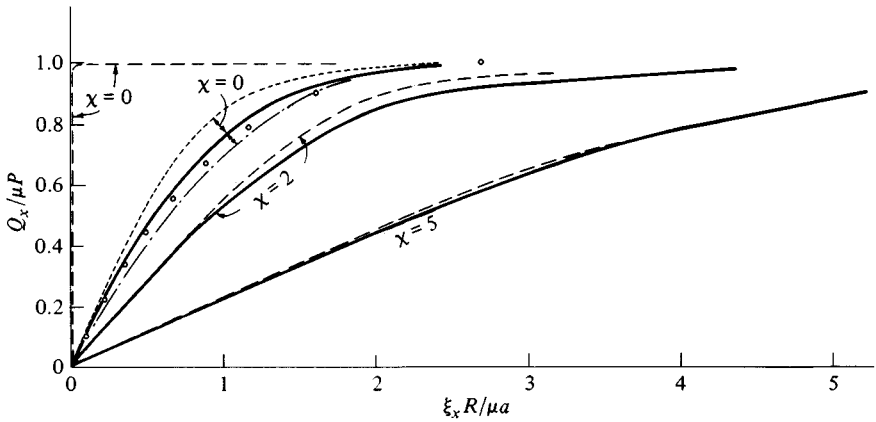

https://doi.org/10.1017/CBO9781139171731.009 Published online by Cambridge University Press

predicts zero creep when $Q_x < \mu P$. With increasing spin, however, it becomes more satisfactory and when $\chi = 5$ it is indistinguishable from Kalker's complete numerical theory.

The case of transverse creep is not so straightforward, since spin itself produces a transverse tangential force, known in the automobile industry as *camber thrust.* In consequence the creep curves are asymmetrical with respect to the origin (Fig. 8.13). This effect is not predicted at all by the theory of complete slip since it is entirely due to tangential elastic compliance of the surface. The complete slip theory, therefore, shows a very large error in this case, even when the spin is large. Once again Kalker's numerical results are well supported by experiment in the range where accurate measurements have been made.

The variation in the transverse force with spin when the transverse creep is zero, i.e. the camber thrust (given by the intersection of the creep curves in Fig. 8.13 with the axis $\xi_y = 0$), is plotted in Fig. 8.14. It rises to a maximum at $(\psi \bar{R}/\mu a) \approx 2$ and falls, with increasing spin, to zero as complete slip is approached. This force arises not only in cornering of a vehicle, but when the axis of rotation of a body is inclined, i.e. 'cambered', to the surface on which it rolls.

Fig. 8.13. Transverse creep combined with spin: theories and experiment (circular contact). Solid line – numerical theory; large-dashed line – complete slip theory; small-dashed line – approximate theory, eq. (8.46).

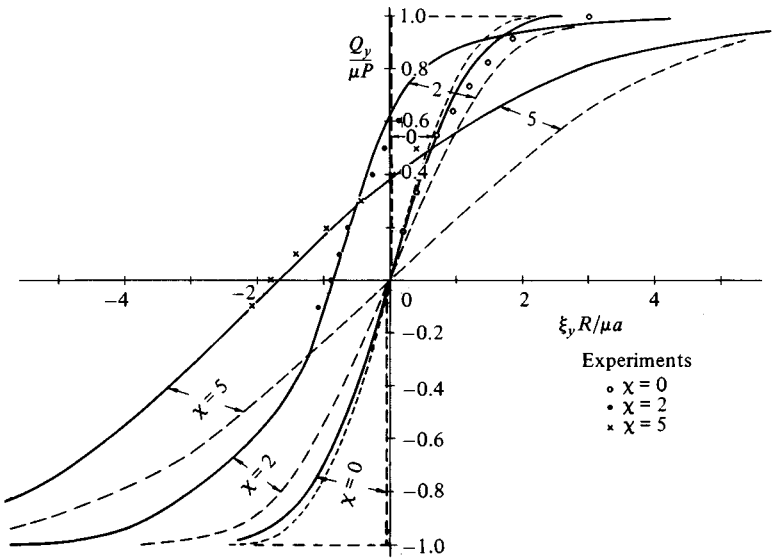

https://doi.org/10.1017/CBO9781139171731.009 Published online by Cambridge University Press

Fig. 8.14. Camber thrust: transverse tangential force due to spin (circular contact). Kalker's numerical theory compared with experiment. Broken line – linear theory, eq. (8.42).

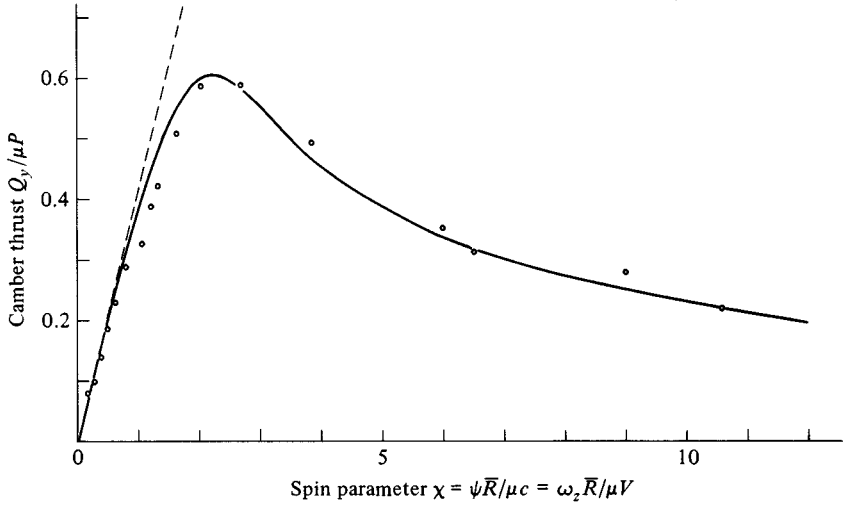

Under engineering conditions, such as are encountered on railway tracks for example, the creep coefficients are observed to be much less than their theoretical values (Hobbs, 1967). A serious cause of this discrepancy lies in the lubricating effect of contaminant films, particularly oil or grease, on the rolling surfaces (Halling & Al-Qishtaini, 1967). Surface roughness and vibration are also likely causes of reduced creep coefficients in practice.

8.5 A ball rolling in a conforming groove

A ball rolling in a groove whose cross-sectional radius of curvature ρ is fairly close to that of the ball itself presents a special case of importance in rolling bearing technology. Under normal load the contact area is an ellipse which is elongated in the transverse direction. With close conformity the contact area is no longer planar but shares the transverse curvature of the ball and groove; surface points in different transverse positions on the ball have different peripheral speeds which leads to micro-slip. To a reasonable approximation the peripheral velocity of the ball is given by

$$V_1 = \omega(R - y^2/2R) \tag{8.54}$$

where R is the radius of the ball, ω is its angular velocity. Thus the creep ratio can be expressed by

$$\xi(y) \equiv \frac{V_1 - V_2}{\omega R} = \left(1 - \frac{V_2}{\omega R}\right) - \frac{y^2}{2R^2} = \xi_0 - y^2/2R^2 \tag{8.55}$$

https://doi.org/10.1017/CBO9781139171731.009 Published online by Cambridge University Press

Under free rolling conditions there is no net tangential force exerted so that the contact area must be split in three zones: a central zone (y small) where the slip is positive and two outer zones (y large) where the slip is negative. Three parallel wear bands were observed in unlubricated ball-bearing races by Heathcote (1921), who developed a theory on the basis of complete slip, i.e. by neglecting the elastic compliance of the ball and race. He deduced that the rotation of the ball would be resisted by a frictional moment M given by

$$\frac{M}{RP} = 0.08\mu \frac{b^2}{R^2} \tag{8.56}$$

where $2b$ is the transverse width of the contact ellipse.

The influence of elastic compliance is not generally negligible however, and can be conveniently analysed by strip theory.

The dimensions of the contact ellipse a and b, and the maximum contact pressure p_0 are given by the Hertz theory. A typical strip is shown in Fig. 8.15 to which the Carter theory is applied. A stick region at the leading edge, whose centre is located at $x = -d$, is followed by a slip region at the trailing edge. Equation (8.24) for the creep ratio of the strip is now substituted into equation (8.55) to give

$$\frac{d}{a} = \Gamma(\gamma^2 - y^2/b^2) \tag{8.57}$$

Fig. 8.15. Strip theory applied to a ball rolling in a conforming groove. Pure rolling takes place on two lines at $y = \pm\gamma b$; elsewhere micro-slip occurs: backwards where $y < \gamma b$ and forwards where $y > \gamma b$.

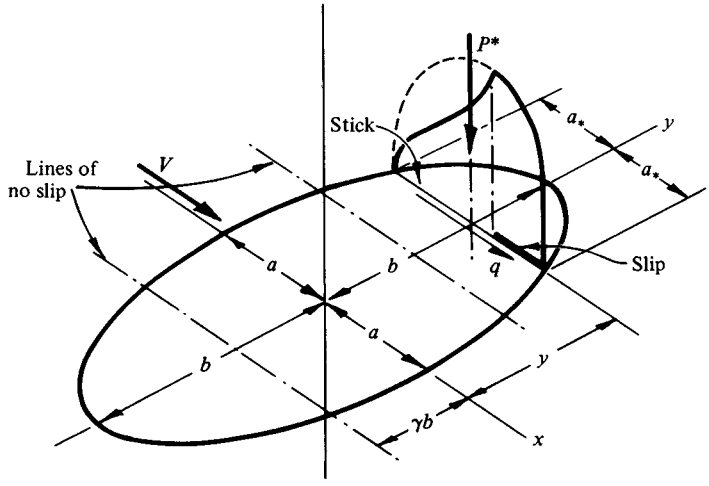

https://doi.org/10.1017/CBO9781139171731.009 Published online by Cambridge University Press

where

$$\Gamma = \frac{b^2 E^*}{4\mu p_0 R^2} = \frac{b^2 \rho \mathbf{E}(e)}{2\mu a R(2\rho - R)}$$

and

$$\gamma^2 = 2R^2 \xi_0 / b^2$$

No micro-slip occurs at $y = \pm\gamma b$ and the extent of slip elsewhere is given by (8.57) provided $d/a_* < 1$. Strips at larger values of y slip completely whereupon $d/a_* = 1$. To determine γ we use the condition of no resultant tangential force. From equation (8.25) the tangential force exerted by the strip per unit width is

$$Q^* = \frac{\pi}{2}\mu p_0^* a_* \frac{d}{a_*}\left(2 - \frac{d}{a_*}\right) = \frac{\pi}{2}\mu p_0 a \frac{d}{a}\left(2\frac{a_*}{a} - \frac{d}{a}\right) \tag{8.58}$$

For free rolling the total traction force

$$Q = \int_{-b}^{b} Q^* \, dy = 0 \tag{8.59}$$

This condition determines the value of γ, the position of the zero slip bands,

Fig. 8.16. Resisting moment on a ball rolling in a conforming groove, eq. (8.60). Broken line – limit for vanishingly small slip; chain line – complete slip, eq. (8.56), Heathcote (1921).

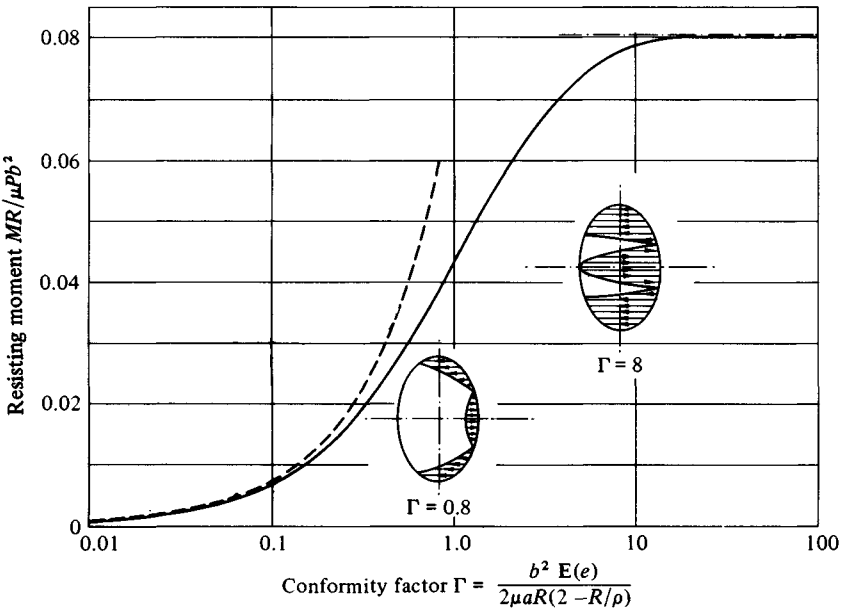

https://doi.org/10.1017/CBO9781139171731.009 Published online by Cambridge University Press

and hence the overall creep ratio ξ_0. The moment resisting rolling is then found by

$$M = \int_{-b}^{b} Q^*(R - y^2/2R)\,\mathrm{d}y = -\int_{-b}^{b} Q^*(y^2/2R)\,\mathrm{d}y \tag{8.60}$$

where the integral is a function of the geometric parameter Γ. The result of computing this integral is shown in Fig. 8.16. When the conformity is close or the coefficient of friction is small, Γ is large, and the moment approaches the result for complete slip given by equation (8.56). Theoretical stick and slip regions are also shown in Fig. 8.16.

8.6 Transient behaviour in rolling

So far in this chapter we have considered the contact stresses which arise in steady rolling, that is when the forces and contact geometry do not change with time and when rolling has proceeded for a sufficient time for the stress field to be no longer influenced by the initial conditions. Various cases of unsteady rolling contact of cylinders in plane strain have been examined in a sequence of papers by Kalker (1969, 1970, 1971*b*).

Since the strain field is changing with time, the term $\partial \bar{u}_x/\partial t$ in equation (8.1*a*) for the particle velocity is no longer zero and appears in the expression for the velocity of slip. In plane strain there is no spin and no motion in the y direction so we can omit the suffix x, and we shall restrict the discussion to similar elastic bodies. Equation (8.3*a*) for the slip velocity then becomes

$$\begin{aligned} \dot{s}(x,t) &= V\xi(t) + 2V\frac{\partial \bar{u}(x,t)}{\partial x} + 2\frac{\partial \bar{u}(x,t)}{\partial t} \\ &= V\xi(t) + 2V\frac{\partial \bar{u}(x,t)}{\partial x} + 2\frac{\partial}{\partial t}(\bar{u}(x,t) - \bar{u}(0,t)) \\ &\quad + \frac{2\partial \bar{u}(0,t)}{\partial t} \end{aligned} \tag{8.61}$$

Difficulty arises in plane strain with the last term in equation (8.61), since the absolute value of $\bar{u}(0,t)$ depends upon the choice of datum for displacements. This choice must be governed by the bulk geometry of the bodies in any particular case. If the length of the contact perpendicular to the rolling direction is well defined and denoted by $2b$ ($b \gg a$), we can take as an approximation to $\bar{u}(0,t)$ the displacement at the centre of a rectangle $2b \times 2a$ due to a uniform traction $q = Q/4a$, i.e.

$$\bar{u}(0,t) = \frac{2(1-\nu^2)Q(t)}{\pi E}\{1/(1-\nu) + \ln(2b/a)\}$$

https://doi.org/10.1017/CBO9781139171731.009 Published online by Cambridge University Press

where Q is the tangential force per unit axial length. The value of $\bar{u}(0, t)$ will not be very sensitive to the precise distribution of traction. In those cases where the normal load, and hence a, remain constant

$$\frac{\partial \bar{u}(0,t)}{\partial t} = \frac{2(1-\nu^2)}{\pi E}\left\{\frac{1}{1-\nu} + \ln\left(\frac{2b}{a}\right)\right\}\frac{\mathrm{d}Q(t)}{\mathrm{d}t} \tag{8.62}$$

This term enters into the calculation of the transient creep; but the difficulty does not arise if the traction only is required.

During rolling we expect the interface to have stick and slip zones governed by the conditions (8.4)–(8.7) in which the slip is now related to the elastic displacements by equation (8.61). The distributions of traction $q(x, t)$ and the value of the creep ratio $\xi(t)$ which satisfy these conditions must be found step by step, starting from given initial conditions, and following the prescribed loading history of the particular problem. The reader is referred to Kalker (1969, 1970, 1971*b*) for the technique of solution; the results of two cases only will be discussed here.

(a) Constant tractive force starting from rest

If a tractive force less than limiting friction is applied to cylinders at rest, micro-slip takes place at both edges of contact and the tangential traction is distributed according to equation (7.28), as shown in Fig. 8.17 ($l = 0$). Assuming no-slip ($\mu \to \infty$) the traction would rise to an infinite value at both edges, given by equation (7.22). The cylinders are now permitted to roll. In the steady-state slip is restricted to the trailing edge and the traction is distributed according to the sum of (7.23) and (8.22). The steady-state traction without slip is given by (8.27). Between the start of rolling and the steady state, the slip regions and tractions vary transiently with l, the distance rolled. Since inertia effects are ignored, $\partial/\partial t = V\partial/\partial l$. The traction distributions at various stages in the process are shown in Fig. 8.17 for the case of no slip ($\mu \to \infty$) and also for the case of partial slip in which $Q = 0.75\mu P$. With no slip the singularity in traction, which is initially located at the leading edge, moves through the contact with the rolling velocity and finally disappears at $l = 2a$ leaving a distribution of traction which is close to that in the steady state. When slip is permitted, the initial application of Q causes slip at both edges but, as rolling proceeds, no further slip occurs at the leading edge. The original traction distribution moves through the contact with the rolling velocity until it merges with the trailing slip zone at $l = 0.6a$. The steady state is virtually reached and established by $l = 1.6a$.

The behaviour might be described qualitatively by saying that the interfacial points, initially located at the leading edge, and their associated traction move

Fig. 8.17. Transient rolling from rest under the action of constant normal and tangential forces: distributions of tangential traction $q(x)$ with distance rolled l. Chain line – no slip ($\mu \to \infty$); solid line – with partial slip ($Q = 0.75\mu P$).

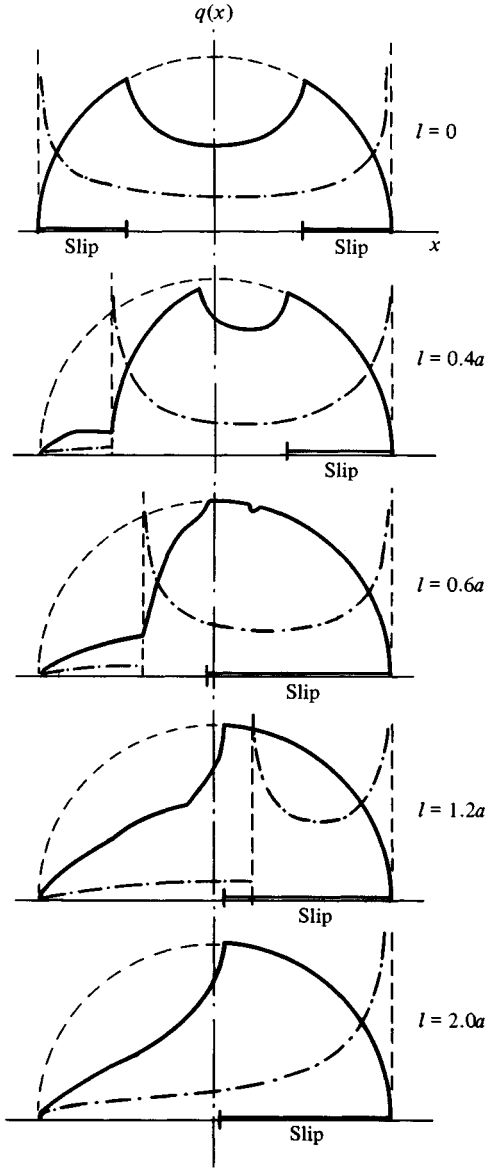

https://doi.org/10.1017/CBO9781139171731.009 Published online by Cambridge University Press

through the contact until they are swallowed up by the slip region at the trailing edge, at which instant a good approximation to the steady state has been reached.

(b) Oscillating tractive force: $Q(t) = Q^* \cos \omega t$

An oscillating tangential force whose period $2\pi/\omega$ is comparable with the time of passage of the surfaces through the contact zone $2a/V$ will induce

Fig. 8.18. Steady cyclic variations of traction due to an oscillating tangential force. $Q(t) = Q^* \cos \omega t$. (*a*) $\omega = V/a$; (*b*) $\omega = 2.405\, V/a$.

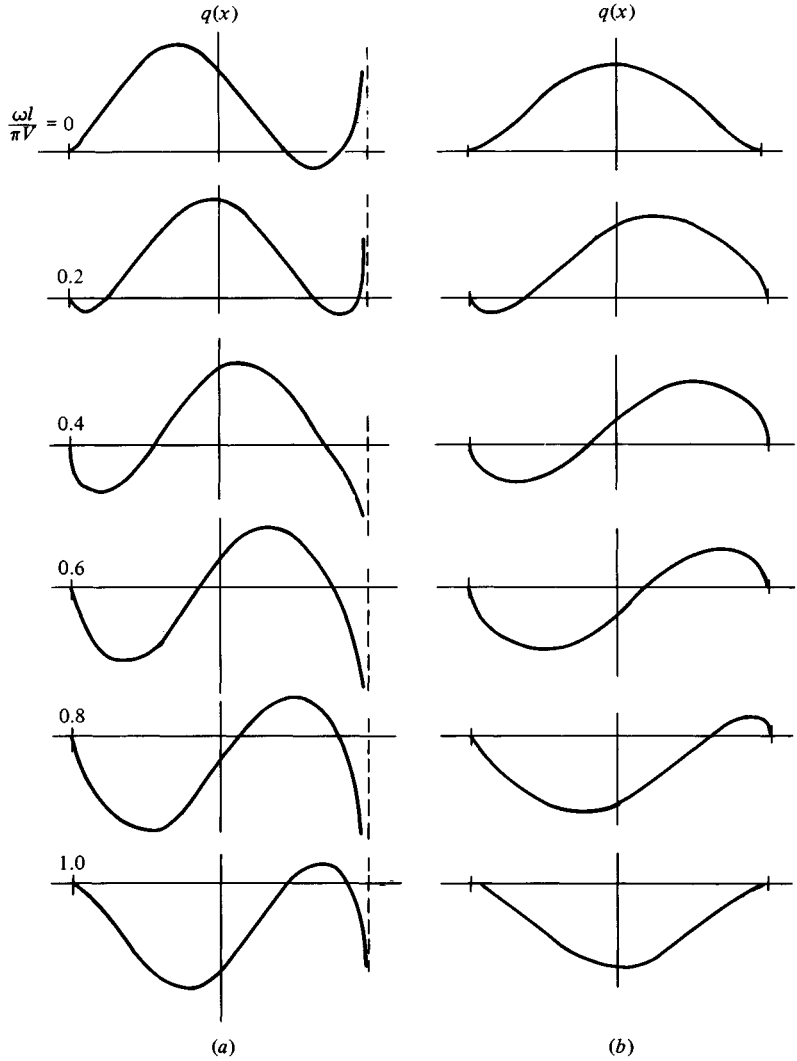

https://doi.org/10.1017/CBO9781139171731.009 Published online by Cambridge University Press

tractions which are appreciably different from those in steady rolling. Transient effects occur at the start, which depend upon the initial state of traction, but after a few cycles the system settles down to a steady cyclic state. By way of example Fig. 8.18(*a*) shows the fifth cycle at a frequency $\omega = V/a$, from which it is evident that a steady cyclic state has been reached in which $q(\omega t + \pi) = -q(\omega t)$. No slip has been permitted in this example and, as expected, an infinite traction oscillating in sign occurs at the trailing edge, which must in fact be relieved by micro-slip. However Kalker has shown that there are a series of specific frequencies ω_n at which no infinite traction arises, given by

$$J_0(\omega_n a/V) = 0 \tag{8.63}$$

where $J_0 \equiv$ Bessel function of the first kind. The traction distributions in the steady cyclic state corresponding to the first such frequency: $\omega_1 = 2.405V/a$, are shown in Fig. 8.18(*b*). Under these conditions no slip occurs at any time provided $Q^*/\mu P$ is less than about 0.4.

The complexities of transient creep analysis have so far restricted exact solutions to two-dimensional cases. Three-dimensional problems involving lateral creep and spin in addition to longitudinal creep can be analysed approximately, however, using the elastic foundation model described in the next section.

8.7 Elastic foundation model of rolling contact

We saw in §4.3 how normal elastic contact could be greatly simplified by modelling the elastic bodies by a simple Winkler elastic foundation rather than by elastic half-spaces. The same expedient can be applied to the tangential tractions which arise in rolling contact. The two rolling bodies can be replaced by a rigid toroid having the same relative principal curvatures, rolling on an elastic foundation of depth h which in turn is supported on a flat rigid substrate. The elasticities of both bodies are represented by the moduli of the foundation: K_p in normal compression and K_q in tangential shear.

The shape and size of the contact ellipse and the contact pressure could be found by the Hertz theory, but it is more consistent to use the elastic foundation model in the manner described in §4.3. The tangential surface displacements $\bar{u}_x$ and $\bar{u}_y$ are related to the components of tangential traction by

$$q_x = (K_q/h)\bar{u}_x; \quad q_y = (K_q/h)\bar{u}_y \tag{8.64}$$

Such a foundation is sometimes referred to as a 'wire brush' model since individual bristles might be expected to deform according to (8.64) independently of their neighbours. The conditions for slip and stick expressed in equations (8.1)–(8.7) still apply and, together with the condition that the

traction is zero on the leading edge, are used to find the distribution of tangential traction throughout the contact area. Since, by (8.64), the traction at any point depends only upon the displacement at that point, the slip equations (8.3) can be integrated directly to find the traction. Under transient conditions the variation in the displacements with time must be followed step by step from the initial conditions to the steady state. The numerical procedure is very straightforward. Kalker (1973) has discussed the procedure in detail with a view to ensuring that the results from the foundation model correspond as closely as possible to exact solutions based on the elastic half-space.

As an example we will consider the tractive rolling contact of long cylinders analysed exactly in §3. The elastic displacements of both surfaces are combined in the displacement $\bar{u}_x$ of the foundation so that in a stick zone equations (8.3) and (8.4) reduce to

$$\xi_x + \frac{\partial \bar{u}_x}{\partial x} = \dot{s}_x/V = 0 \tag{8.65}$$

We can substitute for $\bar{u}_x$ from equation (8.64) to give a simple differential equation for $q(x)$ which, when integrated, with the condition that $q_x = 0$ at $x = -a$, gives

$$q_x = -(K_q \xi_x/h)(a + x) \tag{8.66}$$

Thus the traction increases linearly from the leading edge and, if slip is entirely prevented, it is released suddenly at the trailing edge. In contrast to the exact solution, this traction is still finite at the trailing edge. The total tangential force follows directly from the integration of (8.66) with the result:

$$Q_x = -2K_q \xi_x a^2/h \tag{8.67}$$

In practice slip will occur at the trailing edge where the pressure falls to zero but the traction given by (8.66) does not. For consistency we will take the parabolic pressure distribution given by elastic foundation theory in equation (4.58). A stick region of width $2c$ extends from the leading edge. At the point where slip begins ($x = 2c - a$)

$$q_x = (K_q/h)\xi_x 2c = \mu p = 4\mu(K_p/2Rh)(a - c)c$$

which gives

$$\lambda \equiv 2(1 - c/a) = K_q \xi_x R/K_p \mu a \tag{8.68}$$

The traction force, found from the sum of the traction in both stick and slip zones, is then given by

$$Q_x/\mu P = -\tfrac{3}{2}\lambda(1 - \tfrac{1}{2}\lambda + \tfrac{1}{12}\lambda^2) \tag{8.69}$$

This equation and equation (8.67) are the counterparts of the exact solutions

https://doi.org/10.1017/CBO9781139171731.009 Published online by Cambridge University Press

(8.26) and (8.28); they are compared in Fig. 8.7. In order for the creep coefficient, i.e. the linear gradient, of the foundation model to coincide with that of the half-space solution, the tangential modulus of the foundation K_q should be 2/3 the normal modulus K_p. Thus we should take $K_q a/h \approx 1.1E^*$.†

In a three-dimensional contact undergoing longitudinal creep only, each elemental strip parallel to the x-axis behaves like the two-dimensional contact analysed above. The traction rises linearly from zero at the leading edge until it reaches the value μp when slip starts. If all slip is prevented, integrating the traction over the contact ellipse gives

$$Q_x = \frac{8ab}{3}\left(\frac{K_q a}{h}\right)\xi_x \tag{8.70}$$

To agree with the exact result (8.41) the foundation modulus K_q must be given by

$$\frac{K_q a}{h} = \tfrac{3}{8}GC_{11} = \tfrac{3}{8}(1-\nu)E^*C_{11} \tag{8.71a}$$

where values of C_{11} for different elliptical shapes are quoted in Appendix 5. An identical expression, with C_{11} replaced by C_{22}, is obtained in pure lateral creep. To obtain agreement with exact theory in pure spin requires

$$\frac{K_q a}{h} = \frac{4}{\pi}\left(\frac{b}{a}\right)^{1/2}(1-\nu)E^*C_{23} \tag{8.71b}$$

It is clear that a single value of the foundation modulus will not secure agreement over the whole range of creep conditions or (b/a). However, if we take $(K_q a/h) = 1.1E^*$, as in the two-dimensional case, equation (8.71a) gives (for $\nu = 0.3$) $C_{11} = C_{22} = 4.2$ and equation (8.71b) gives $C_{23} = 1.2(a/b)^{1/2}$ which compare reasonably with the values in the table except where $b \ll a$.

If, in the case of pure longitudinal or lateral creep, slip is assumed to occur when the tangential traction reaches its limiting value μp (where p is given by eq. (4.54)) the boundary between the stick and slip regions is found to be a reflexion of the leading edge as observed by experiment.

8.8 Pneumatic tyres

A wheel having a pneumatic tyre is an elastic body which, in rolling contact with the ground, exhibits most of the phenomena of creep and micro-slip which have been discussed in this chapter. In fact, the tangential force and twisting moment due to lateral creep, usually referred to as the 'cornering

† Although we can use the combined modulus E^* to account for the elasticities of both bodies, the foundation model is incapable of handling the tractions which arise from a *difference* in their elastic properties as discussed in § 2.

https://doi.org/10.1017/CBO9781139171731.009 Published online by Cambridge University Press

force' and 'self-aligning torque' play a significant role in the steering characteristics of a road vehicle. Clearly the complex structure of a tyre does not lend itself to the analytical treatment which is possible for solid isotropic bodies; nevertheless simple one-dimensional models have been proposed which do account for the main features of the observed behaviour.

A thin flexible membrane of toroidal shape with internal pressure, when pressed into contact with a rigid plane surface, has a contact area whose approximately elliptical shape is related to the intersection of the plane with the undeformed surface of the toroid and whose area is sufficient to support the contact force by the internal pressure. An aircraft tyre, which has very little tread, approximates to a thin membrane. Referring to Fig. 8.19 the apparent dimensions of the contact ellipse a' and b' are related to the vertical deflexion of the wheel by

$$a' = \{(2R - \delta)\delta\}^{1/2}, \quad b' = \{(w - \delta)\delta\}^{1/2}$$

The apparent area of contact is

$$a'b' = \pi\delta\{(w - \delta)(2R - \delta)\}^{1/2} 2\pi wR\delta \tag{8.72}$$

In reality the tyre is tangential to the flat surface at the periphery of the contact, so that the real contact dimensions a and b are less than a' and b'. The true area is found to be about 85% of the apparent value; the deflexion is found to be approximately proportional to the load with 80–90% of the load taken by the inflation pressure. The stiff tread and cross-section shape of a motor tyre, on the other hand, result in a contact path which is roughly rectangular, having a constant width equal to the width of the tread and having slightly rounded ends. The load is transmitted from the ground to the rim through the walls as shown in Fig. 8.20. When the ground reaction P is applied to the tyre the tension

Fig. 8.19. A pneumatic tyre as a thin inflated membrane.

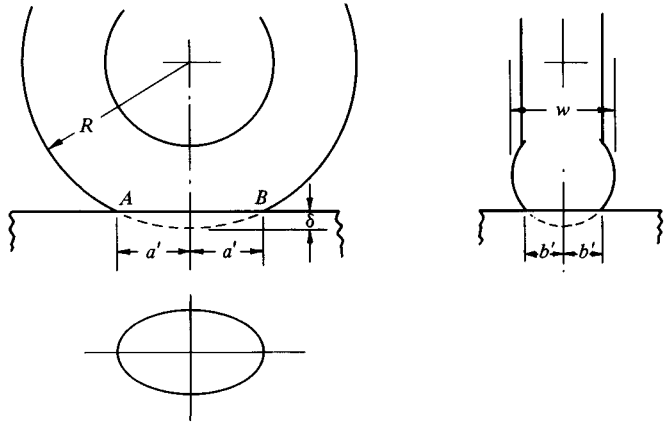

https://doi.org/10.1017/CBO9781139171731.009 Published online by Cambridge University Press

in the walls is decreased with a consequent increase in curvature, thereby exerting an effective upthrust on the hub.

On the membrane model the contact pressure distribution would be uniform and equal to the inflation pressure, whereas a solid tread would concentrate the pressure in the centre. The effect of bending stiffness of the tread is to introduce pressure peaks at the ends of the contact (see §5.8) and support from the walls gives high pressures at the edge. The relative importance of these different effects depends upon the design of tyre.

Creep in free rolling

Like a solid elastic wheel in contact with a rigid ground, a pneumatic tyre will exhibit longitudinal creep if the circumferential strain in the contact patch is different from that in the unloaded periphery. Following membrane theory, the centre-line of the running surface is shortened in the contact patch by the difference between the chord AB and the arc AB. By geometry this gives a strain, and hence a creep ratio:

$$\xi_x = \frac{\partial u_x}{\partial x} = -\delta/3R \tag{8.73}$$

This equation assumes that behaviour of the whole contact is governed by the centre-line strain and that there is no strain outside the contact, therefore the fact that it agrees well with observations must be regarded as somewhat fortuitous.

Transverse tangential forces from sideslip and spin

When the plane of a wheel is slightly skewed to the plane of rolling, described as 'sideslip' or 'yaw', transverse friction forces and moments are

Fig. 8.20. Contact of an automobile tyre with the road: (*a*) unloaded, (*b*) loaded.

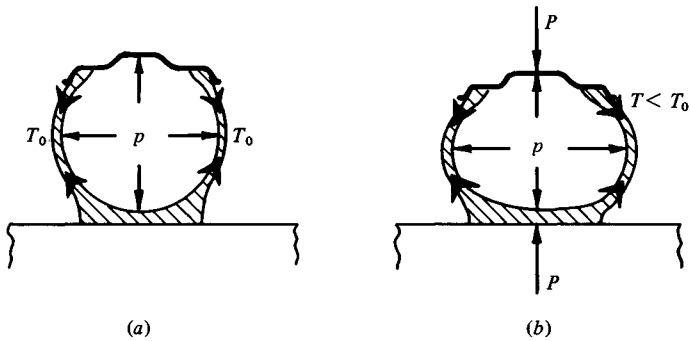

https://doi.org/10.1017/CBO9781139171731.009 Published online by Cambridge University Press

brought into play; they also arise owing to spin when turning a corner or by cambering the axis of the wheel at an angle to the ground. The behaviour is qualitatively the same as that for solid bodies discussed in §4. The contact is divided into a stick region at the leading edge of the contact patch and a slip region at the trailing edge. The slip region spreads forward with increasing sideslip or spin.

A one-dimensional model of the resistance of a tyre to lateral displacement is shown in Fig. 8.21. The lateral deformation of the tyre is characterised by the lateral displacement u of its equatorial line, which is divided into the displacement of the carcass u_c and that of the tread u_t. Owing to the internal pressure the carcass is assumed to carry a uniform tension T. This tension resists lateral deflexion in the manner of a stretched string. Lateral deflexion is also restrained by the walls, which act as a spring foundation of stiffness K per unit length. The tread is also assumed to deflect in the manner of an elastic foundation ('wire brush') as discussed in §7. The tyre is deflected by a transverse surface traction $q(x)$ exerted in contact region $-a \leqslant x \leqslant a$. The equilibrium equation is:

$$K_c u_c - T\frac{\partial^2 u_c}{\partial x^2} = q(x) = K_t u_t \tag{8.74}$$

where K_t is the tread stiffness. The lateral slip velocity in the contact region is given by equation (8.3*b*). The ground is considered rigid ($u_2 = 0$) and the motion one-dimensional, so that we can drop the suffixes. Thus

$$\dot{s}/V = \xi + \psi(x/a) + \frac{\mathrm{d}u}{\mathrm{d}x} \tag{8.75}$$

Fig. 8.21. The 'stretched string' model of the lateral deflexion of a tyre. The carcass and the tread resist lateral deflexion as elastic foundations of stiffness K_c and K_t.

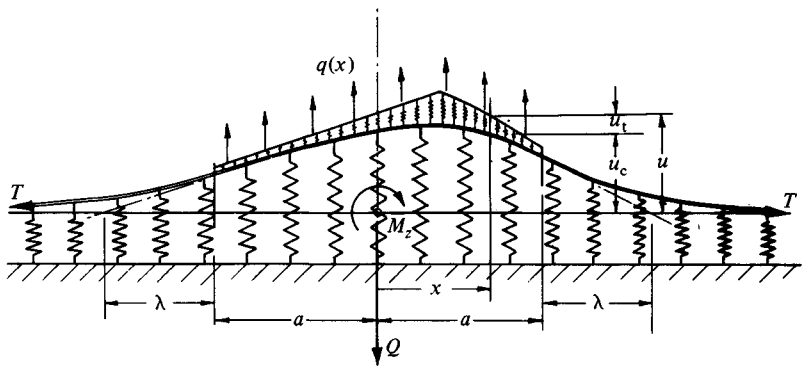

https://doi.org/10.1017/CBO9781139171731.009 Published online by Cambridge University Press

In a stick region $\dot{s} = 0$.

Various approaches to the solution of the problem have been proposed. Fromm (1943) took the carcass to be rigid ($u_c = 0$) so that all the deformation was in the tread ($u = u_t$). Equations (8.74) and (8.75) can then be solved directly throughout the contact region for any assumed pressure distribution. The carcass deflexions are clearly not negligible however and it is more realistic to follow von Schlippe (1941) and Temple (see Hadekel, 1952) who neglected the tread deflexion compared with the carcass deflexion ($u_t = 0, u = u_c$) as shown in Fig. 8.22. Equation (8.74) then becomes

$$u - \lambda^2 \frac{d^2u}{dx^2} = q(x)/K_c \tag{8.76}$$

where the 'relaxation length' $\lambda = (T/K_c)^{1/2}$. To develop a linear theory we shall assume vanishingly small slip, so that in equation (8.75) $\dot{s} = 0$ throughout the contact region. Taking the case of sideslip first, from (8.75) the displacement within the contact region is given by

$$u = u_1 - \xi x$$

where u_1 is the displacement at the leading edge ($x = -a$). Outside the contact region $q(x) = 0$ so that the complementary solution to (8.76) gives

$$u = u_1 \exp\{(a + x)/\lambda\}$$

ahead of the contact and

$$u = u_2 \exp\{(a - x)/\lambda\}$$

at the back of the contact.

Fig. 8.22. Traction distribution for a tyre with yaw angle ξ and no slip in the contact patch: von Schlippe's theory.

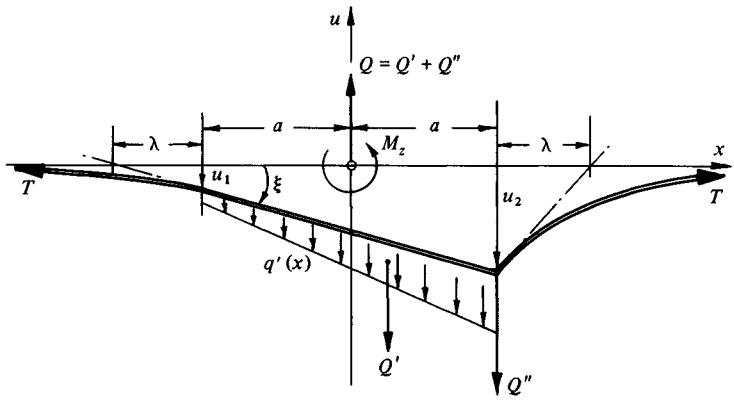

https://doi.org/10.1017/CBO9781139171731.009 Published online by Cambridge University Press

From our discussions in §4 of the location of slip and stick regions, it is clear that the displacement gradient must be continuous at the leading edge, for which $u_1 = -\lambda\xi$. The deflected shape of the equatorial line is shown in Fig. 8.22 together with the traction distribution. In the contact patch itself

$$q'(x) = K_c u = -K_c\xi(\lambda + a + x)$$

which corresponds to a force $Q' = -2K_c a(\lambda + a)$. At the trailing edge ($x = a$) the discontinuity in du/dx gives rise to an infinite traction $q''(a)$ which corresponds to a concentrated force Q'' of magnitude $-2K_c\xi\lambda(\lambda + a)$. The total cornering force is thus

$$Q = Q' + Q'' = -2K_c\xi a^2\left(\frac{\lambda}{a} + 1\right)^2 \tag{8.77}$$

Taking moments about O gives the self-aligning torque to be

$$M_z = \int_{-a}^{a} q(x)x\,dx = -2K_c\xi a^3\left(\tfrac{1}{3} + \frac{\lambda}{a} + \frac{\lambda^2}{a^2}\right) \tag{8.78}$$

As with solid bodies, the infinite traction at the trailing edge necessitates slip such that the deflected shape $u(x)$ has no discontinuity in gradient and satisfies the condition $q(x) = \mu p(x)$ within the slip region. Calculations of the cornering force Q and self-aligning torque M_z by Pacejka (1981) assuming a parabolic pressure distribution and taking $\lambda = 3a$ are shown in Fig. 8.23.

Fig. 8.23. Cornering force Q and self-aligning torque M_z by von Schlippe's theory ($\lambda = 3a$) from Pacejka (1981). Broken line – linear theory (no slip), eqs. (8.77), (8.78).

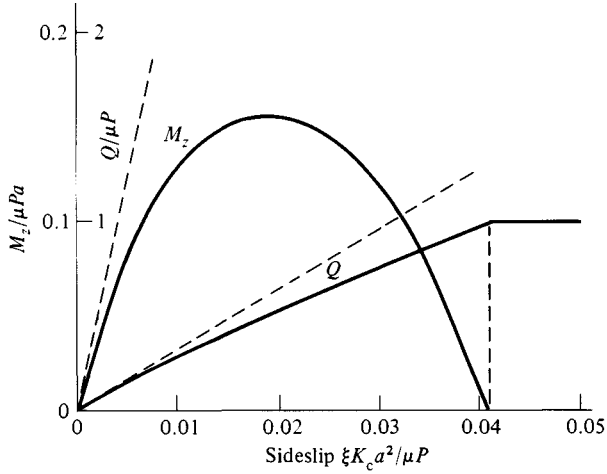

https://doi.org/10.1017/CBO9781139171731.009 Published online by Cambridge University Press

In the case of pure spin, equations (8.75) demands that the deflected shape in the stick region should be parabolic, i.e.

$$u = u_1 + \psi x^2/a$$

Proceeding as before to ensure continuity at $x = -a$ leads to a distribution of traction and to a resultant transverse force ('camber thrust')

$$Q = -2K_c\psi a^2\left(\tfrac{1}{3} + \frac{\lambda}{a} + \frac{\lambda^2}{a^2}\right) \quad \text{and} \quad M_z = 0 \tag{8.79}$$

Equations (8.77)-(8.79) are equivalent to the linear (small slip) equations (8.41)-(8.43) for solid bodies.

The analysis outlined above has been extended by Pacejka (1981) to include the elasticity of the tread. Some investigators have felt that the representation of the carcass by a 'string' in tension is inadequate and have included a term proportional to (d^4u/dx^4) in the equilibrium equation (8.74) to represent the flexural stiffness of the carcass (see Frank, 1965). However the influence on the overall conclusions of the theory is relatively minor since the values of the elasticity parameters of the tyre (K_c, K_t, λ etc.) have to be found by experiment rather than directly from the structure of the tyre.

Longitudinal creep due to driving or braking can be analysed in the same way. If the cover is regarded as an 'elastic belt' restrained circumferentially by the elastic walls, an equilibrium equation similar to (8.75) is obtained for the circumferential displacements of the belt. Recent reviews of tyre mechanics have been published by Clark (1971) and by Pacejka & Dorgham (1983).